Renewable Energy
Power for a sustainable future

Fourth Edition
Stephen Peake

Oxford University Press 2018
ISBN 978-0-19-875975-1

Chapter 8 distributed at DTU course Introduction to Future Energy 47202 as part of the Wind Energy lecture

Chapter 8

Wind energy

By Derek Taylor

8.1 Introduction

Wind energy has been used for thousands of years for milling grain, pumping water and other mechanical power applications. Today, there are many thousands of windmills in operation around the world, a proportion of which are used for water pumping. But it is the use of wind energy as a pollution-free means of generating electricity on a significant scale that is attracting most current interest in the subject. Strictly speaking, a wind*mill* is used for milling grain, so modern technology for electricity generation is generally differentiated by use of the term **wind turbines**, partly because of their functional similarity to the steam and gas turbines that are used to generate electricity, and partly to distinguish them from their traditional forebears. Wind turbines are also sometimes referred to as **wind energy conversion systems (WECS)** and sometimes described as **wind generators** or **aerogenerators**.

Attempts to generate electricity from wind energy have been made (with various degrees of success) since the late nineteenth century when Professor James Blyth of the Royal College of Science and Technology, now Strathclyde University, built a range of wind energy devices to generate electricity, his first being in 1887. A later design built at Marykirk in Scotland continued to generate electricity for over 20 years. In 1888 Professor Charles Brush built a 12 kW wind generator, based on a 50 m diameter, 19th century multiblade style, horizontal axis wind turbine that ran for 20 years. In 1891 Professor Poul la Cour began experimenting with an electricity generating windmill to produce and store hydrogen. This was to be used for lighting at Askov Folk High School in Denmark. He later initiated the Danish Wind Electricity Society (DVES) in 1903 and his experiments became the foundation of the Danish wind energy industry.

For many years, small-scale wind turbines have been manufactured to provide electricity for remote houses, farms and remote communities, and for charging batteries on boats, caravans and holiday cabins (thousands of small turbines similar to that shown in Figure 8.1 are in use worldwide). More recently they have been used to provide electricity for cellular telephone masts, traffic signs, street lighting and remote telephone boxes.

Figure 8.1 The Marlec Rutland 1200 Windcharger which can generate up to 500 watts (source: Marlec, 2016)

However, it is only since the 1980s that the technology has become sufficiently mature to enable rapid growth of the sector. Between the early 1980s and the late 2000s the cost of wind turbines fell steadily and the rated capacity of typical machines increased significantly. Now, on reasonably windy and accessible sites, wind turbines are one of the most cost-effective methods of electricity generation. Given continuing improvements in cost, capacity and reliability, it can be expected that wind energy will become even more economically competitive over the coming decades. Moreover, as wind turbines are increasingly deployed offshore, where wind speeds are generally higher and planning constraints perhaps less demanding, the technically accessible wind resource is massively increased. Of course, as will be seen later, there are significant additional technical challenges associated with offshore wind and the cost of generation is inevitably higher.

The improvements in wind power technology have made it one of the fastest growing renewable energy technologies worldwide in terms of installed rated capacity. A total of over 432 GW of wind generating capacity had been installed by the end of 2015, with almost 36 GW added in that year. This is about 24 times the capacity that had been installed by the end of 2000, and, at the time of writing, the current average growth rate is around 17% cumulatively and 22% per annum. In June 2017, global wind power capacity went past half a terawatt (500 GW).

To understand the machines and systems that extract energy from the wind involves an appreciation of many fields of knowledge, from meteorology, aerodynamics and planning to electrical, structural, civil and mechanical engineering. Hence, this chapter begins with a description of the atmospheric processes that give rise to wind energy. Wind turbines and their aerodynamics are then described, together with various ways of calculating their power and energy production. This is followed by discussions of the environmental impact and economics of wind energy, together with an examination of recent commercial developments and a discussion of its future potential. The final section looks at offshore wind power, which seems likely to be one of the most important areas of wind energy development in coming decades, especially for the UK and northern Europe.

8.2 The wind

As mentioned in Chapter 3, one square metre of the Earth's surface on or near the equator receives more solar radiation per year than one square metre at higher latitudes. The curvature of the Earth means that its surface becomes more oblique to the Sun's rays with increasing latitude. In addition, the Sun's rays have further to travel through the atmosphere as latitude increases, so more of the Sun's energy is absorbed *en route* before it reaches the surface. As a result of these effects, the tropics are considerably warmer than higher latitude regions.

This differential solar heating of the Earth's surface causes variations in atmospheric pressure, which in turn give rise to the movement of atmospheric air masses which are the principal cause of the Earth's wind systems (see Box 8.1 for more details).

BOX 8.1 The Earth's wind systems

Like all gases, air expands when heated, and contracts when cooled. Thus warm air is less dense than cold air and will rise to high altitudes when strongly heated by solar radiation.

A low pressure belt (with cloudy and rainy weather patterns) is created at the equator due to warm humid air rising in the atmosphere until it reaches the tropopause (the top of the troposphere). At the surface the equatorial region is called the 'doldrums' (from an old English word meaning dull) by early sailors who were fearful about becoming becalmed.

At the tropopause in the northern hemisphere the air moves northwards and in the southern Hemisphere it moves southwards. This air gradually cools until it reaches latitudes of about 30 degrees, where it sinks back to the surface, creating a belt of high pressure at these latitudes (with dry clear weather patterns). The majority of the world's deserts also occur in these high-pressure regions.

Some of the air that reaches the surface at these latitudes is forced back towards the low-pressure zone at the equator. These air movements are known as the '**trade winds**'. On reaching the equator these air movements complete the circulation of what is known as the **Hadley cell** – named after the scientist (George Hadley) who first described them in 1753.

However, not all of the air that sinks at the 30 degree latitudes moves toward the equator. Some of it moves poleward until it reaches the 60 degree latitudes, where it meets cold air coming from the poles at what are known as the 'polar fronts'. The interaction of the two bodies of air causes the warmer air to rise and most of this air cycles back to the 30-degree latitude regions where it sinks to the surface, contributing to the high-pressure belt. This completes the circulation of what is known as the **Ferrel cell** (named after William Ferrel who first identified it in 1856).

The remaining air that rises at the polar fronts moves poleward and sinks to the surface at the poles as it cools. It then returns to the 60-degree latitude region completing the circulation of what is known as the **polar Hadley cell** or **polar cell**.

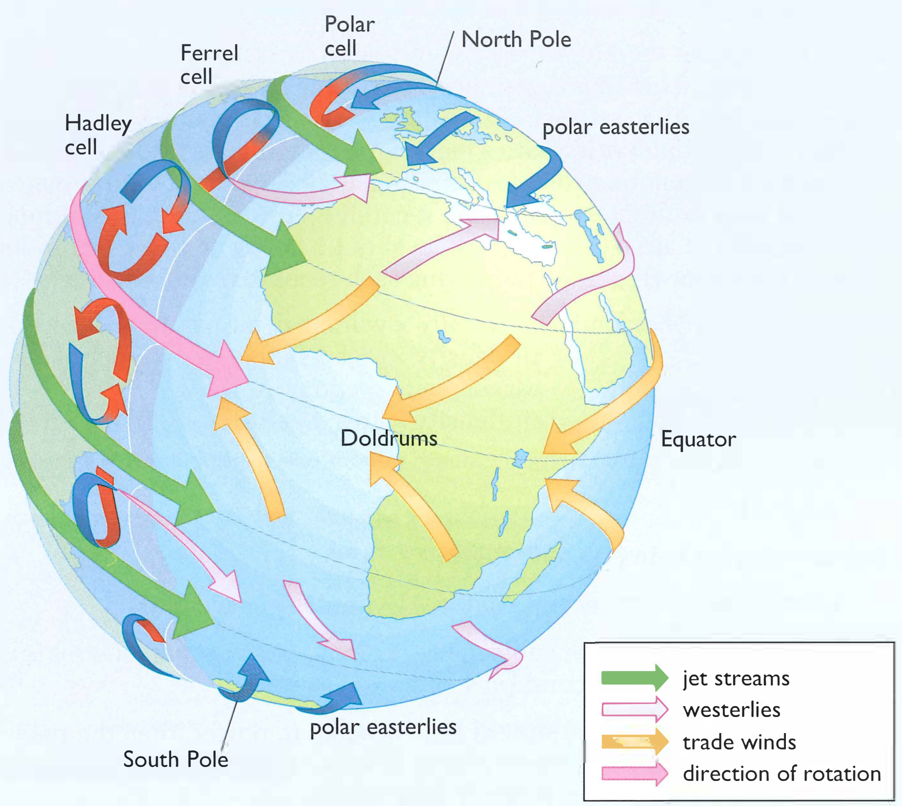

Figure 8.2 The global wind circulation (source: Burroughs et al., 1996)

There is a further complication in that, because the Earth itself rotates, winds moving across the Earth's surface are subject to a phenomenon known as the Coriolis Effect. The net result of this effect, given the Earth rotates in an eastwards direction, is that in the northern hemisphere 'north bound' winds are caused to veer 'right'. Such winds are known as 'westerlies' as, whilst they are veering toward an easterly direction, it is the convention when referring to wind direction to use the direction from which winds blow. In the southern hemisphere 'north bound' winds veer to the 'left' ('trade winds'). Likewise, 'south bound' winds veer 'right' ('trade winds') in the northern hemisphere and 'left' ('westerlies') in the southern hemisphere. Figure 8.2 shows the overall pattern of global wind circulation.

Atmospheric pressure is the pressure resulting from the weight of the column of air above a specified surface area, with the unit of atmospheric pressure being known as the bar. Atmospheric pressure is measured by means of a barometer (Figure 8.3). These devices are usually calibrated in millibars (mbar), that is, thousandths of a bar. The average atmospheric pressure at sea level is about 1013.2 mbar (approximately 1 bar). The SI unit of pressure, the pascal (Pa), is defined as one newton per square metre and 1 bar is equivalent to 100 kPa.

On the weather maps featured in television weather forecasts or in newspapers, there are regions marked 'high' and 'low', surrounded by contours (Figure 8.4). The regions marked 'high' and 'low' relate to the atmospheric

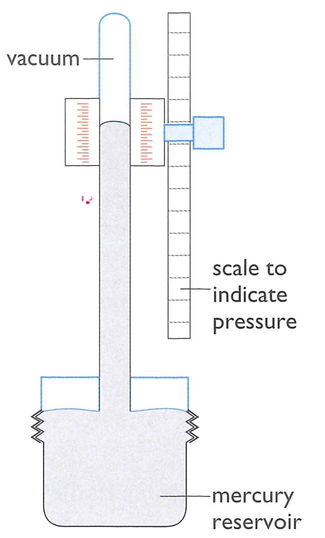

Figure 8.3 A Fortin barometer, an example of a barometer used to measure atmospheric pressure. Variations in atmospheric pressure acting on the mercury in the reservoir cause the mercury in the column to rise or fall

pressure and the contours represent lines of equal pressure called **isobars**. The high-pressure regions tend to indicate fine weather with little wind, whereas the low-pressure regions tend to indicate changeable windy weather and precipitation.

In addition to the main global wind systems shown in Box 8.1 there are also local wind patterns, such as sea breezes (Figure 8.5) and mountain valley winds (Figure 8.6).

Energy and power in the wind

The energy contained in the wind is its kinetic energy, and as we saw in Chapter 1 the kinetic energy of any particular moving mass (moving air in this case) is equal to half the mass, m, (of the air) times the square of its velocity, V:

$$\text{kinetic energy} = \text{half mass} \times \text{velocity squared} = \frac{1}{2}mV^2 \qquad (1)$$

where m is in kilograms and V is in metres per second (m s^{-1}).

We can calculate the kinetic energy in the wind if, first, we imagine air passing through a circular ring or hoop enclosing an area A (say 100 m^2) at a velocity V (say 10 m s^{-1}) (see Figure 8.7). As the air is moving at a velocity of 10 m s^{-1}, a cylinder of air with a length of 10 m will pass through the ring each second. Therefore, a volume of air equal to 10 × 100 = 1000 cubic metres (m^3) will pass through the ring each second. By multiplying this volume by the density of air, ρ (which at sea level is 1.2256 kg m^{-3}), we obtain the mass of the air moving through the ring each second. In other words:

$$\begin{aligned} \text{mass } (m) \text{ of air per second} &= \text{air density} \times \text{volume of air passing per second} \\ &= \text{air density} \times \text{area} \times \text{length of cylinder of air passing per second} \\ &= \text{air density} \times \text{area} \times \text{velocity} \end{aligned}$$

that is:

$$m = \rho AV$$

Substituting for m in (1) above gives:

$$\text{kinetic energy per second} = 0.5\,\rho AV^3 \text{ (joules per second)}$$

where ρ is in kilograms per cubic metre (kg m^{-3}), A is in square metres (m^2) and V is in metres per second (m s^{-1}).

If we recall that energy per unit of time is equal to power, then the power in the wind is P (watts) = kinetic energy in the wind traversing the circular ring per second (joules per second), that is:

$$P = 0.5\,\rho AV^3 \qquad (2)$$

The main relationships that are apparent from the above calculations are that the power in the wind is proportional to:

- the density of the air
- the area through which the wind is passing (i.e. through a wind turbine rotor), and
- the cube of the wind velocity.

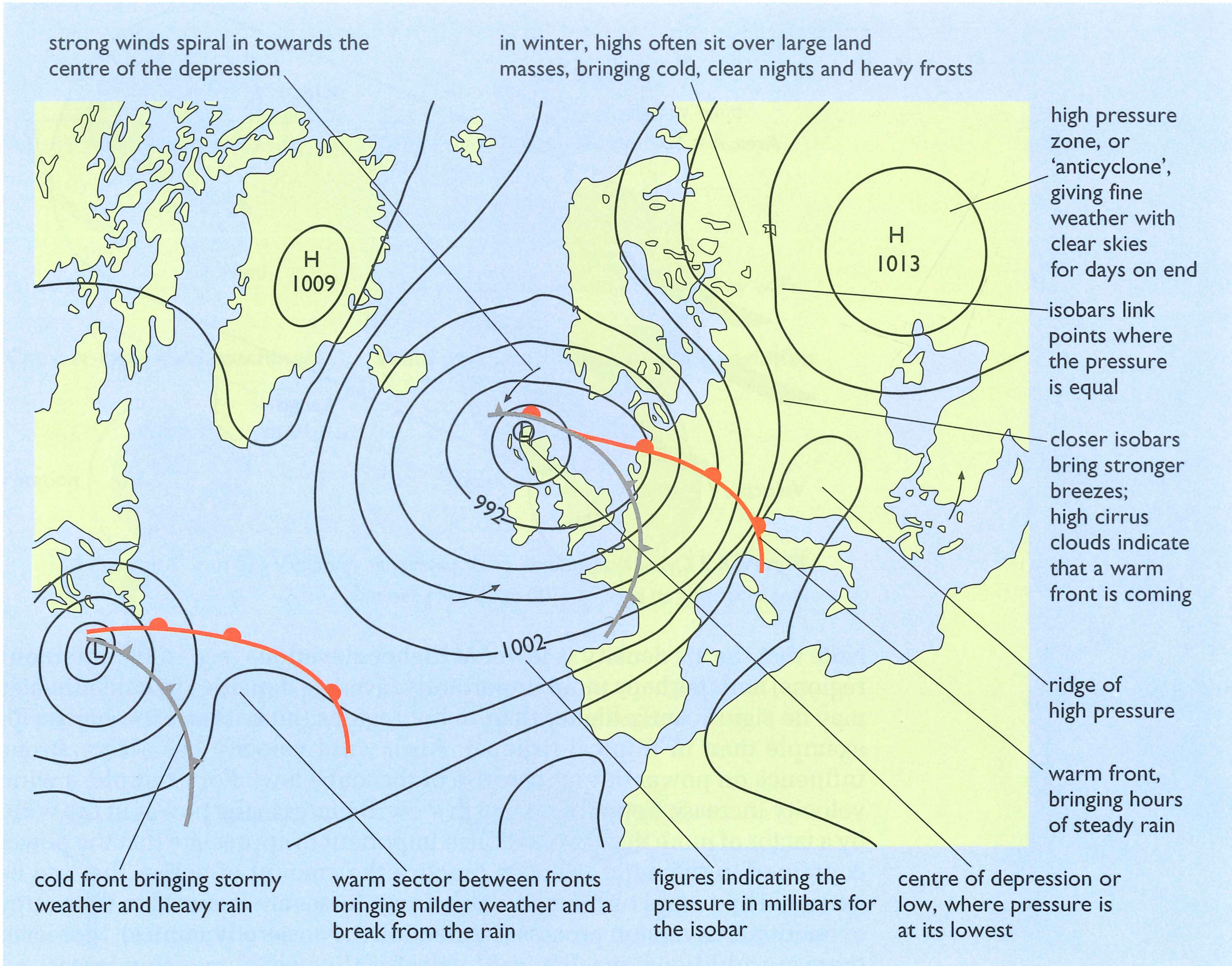

Figure 8.4 Typical weather map showing regions of high (H) and low (L) pressure

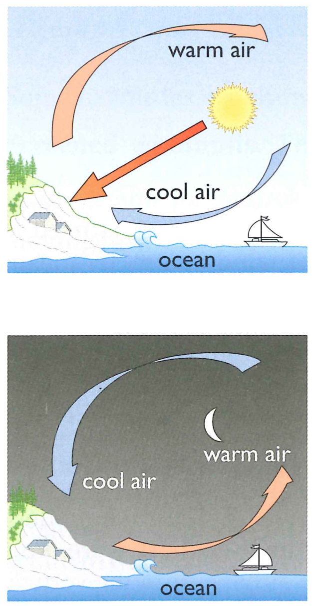

Figure 8.5 Sea breezes are generated in coastal areas as a result of the different heat capacities of sea and land, which give rise to different rates of heating and cooling. The land has a lower heat capacity than the sea and heats up quickly during the day, but at night it cools more quickly than the sea. During the day, the sea is therefore cooler than the land and this causes the cooler air to flow shoreward to replace the rising warm air on the land. During the night the direction of air flow is reversed

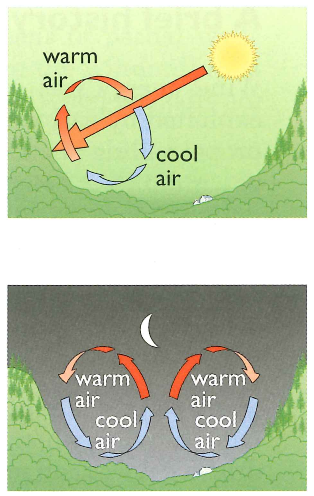

Figure 8.6 Mountain valley winds are created when cool mountain air warms up in the morning and, as it becomes lighter, begins to rise: cool air from the valley below then moves up the slope to replace it. During the night the flow reverses, with cool mountain air sinking into the valley

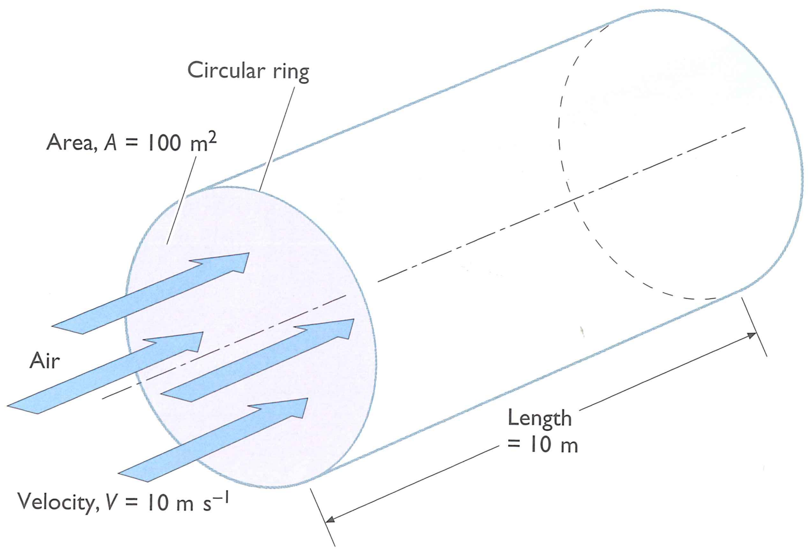

Figure 8.7 Cylindrical volume of air passing at velocity V (10 m s^{-1}) through a ring enclosing an area, A (100 m^{-2}), each second

Note that the air density is lower at higher elevations (e.g. in mountainous regions) and, perhaps more importantly, average densities in cold climates may be significantly higher than in hot regions (more than 10% higher for example than in tropical regions). Also, wind velocity has a very strong influence on power output because of the 'cube law'. For example, a wind velocity increase from 6 m s^{-1} to 8 m s^{-1} will increase the power in the wind by a factor of more than two. It is also important to appreciate that the power contained in the wind is not in practice the amount of power that can be extracted by a wind turbine. This is because losses are incurred in the energy extraction/conversion process (see Section 8.4 on aerodynamics). Moreover there are additional mechanical-to-electrical power conversion losses.

8.3 Wind turbines

A brief history of wind energy

Wind energy was one of the first non-animal sources of energy to be exploited by early civilizations. It is thought that wind was first used to propel sailing boats, but the static exploitation of wind energy by means of windmills is believed to have been taking place for about 4000 years.

Windmills have traditionally been used for milling grain, grinding spices, dyes and paint stuffs, making paper and sawing wood. Traditional wind pumps were used for pumping water in Holland and East Anglia in the UK, and, because they often used identical forms of sails and support structures, they were (and are) often also referred to as windmills.

Many early windmills were of the *vertical-axis* type and, unlike modern wind turbines which are driven by lift forces (see below), these were drag-driven devices and relied on differences in drag on either side of the vertical shaft in order to function.

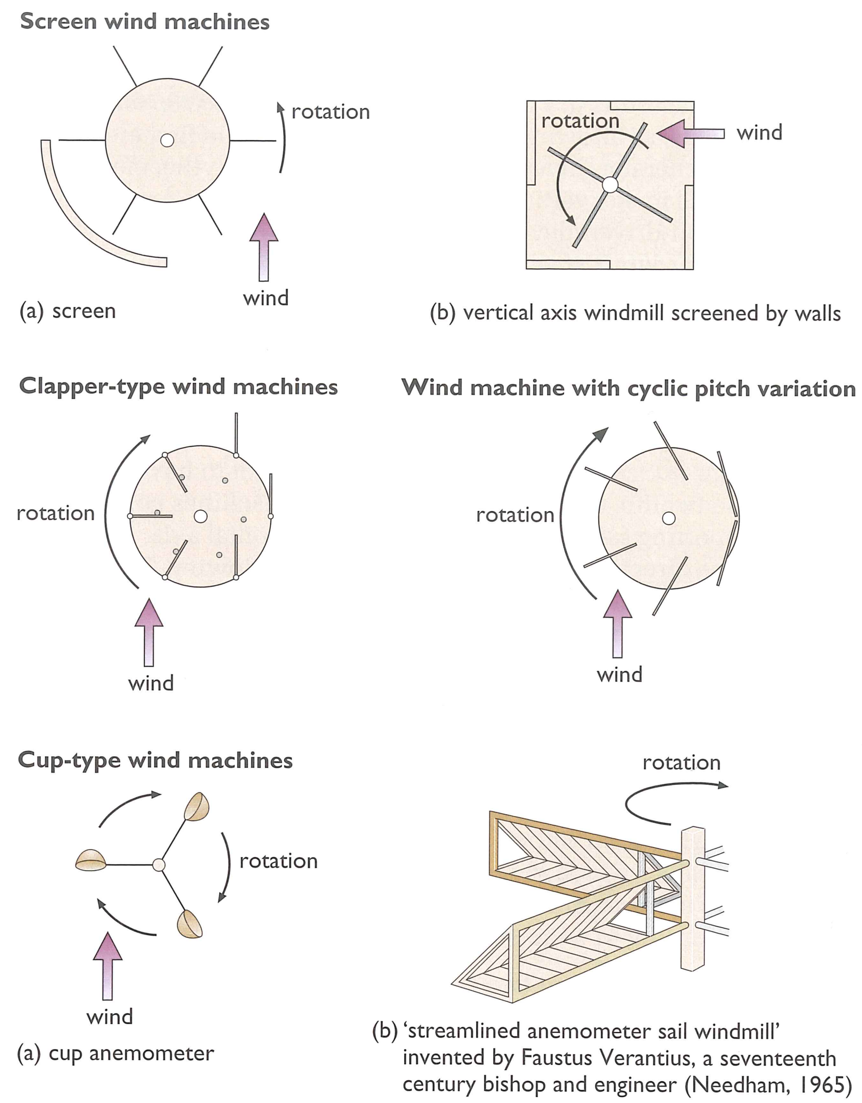

Figure 8.8 Some examples of traditional vertical-axis windmills

Some examples are shown in Figure 8.8 and include the following.

Screened windmills. These windmills employ screens or partial walls around the windmill, which are positioned to screen the windmill sails from the wind during the 'backward' part of the cycle, when the sails are moving towards the wind.

'Clapper' windmills. These windmills are so called because the moveable sails 'clap' against stops as the rotor turns with the wind (forwards), maximizing their air resistance, but align themselves with the wind (like a weather vane) when on the part of their cycle in which they are moving into the wind (backwards), so reducing their air resistance.

Cyclically pivoting sail windmills. These windmills are similar to the 'clapper' windmills, but use a more complex mechanism to achieve progressive changes in sail orientation. The pitch angle of each sail is cyclically adjusted according to its position during its rotation cycle and to the direction of the wind. This gives a difference in resistance on either side of the windmill's rotation axis, causing it to rotate when exposed to a wind stream.

Differential resistance or cup type windmills. In these windmills, the blades are shaped to offer greater resistance to the wind on one surface compared with the other. This results in a difference in wind resistance on either side of the windmill axis, so allowing the windmill to turn. The first electricity producing wind generator, invented by Professor James Blythe, mentioned above, was a 10 m diameter vertical axis cup type device. A modern example of this type of wind-driven device is the cup anemometer, an instrument used for measuring wind speed. The simple 'S' type and multi-bladed S-type windmills are also examples of this type, as is the 'Savonius rotor' (a 'split-S' shaped rotor as shown in Figure 8.9). Savonius rotors are used for powering fans in trucks and vans and have been used for simple do-it yourself windmills. They are produced as micro wind generators, including variants with helically twisted semi-cylindrical 'cups'.

The more familiar *horizontal-axis* windmills are thought to have appeared in Europe in the twelfth century. These traditional machines consisted of radial arms supporting sails that rotated about a horizontal axis, in a plane that faced into the direction from which the wind was blowing. The sails or blades themselves were set at a small oblique angle to the wind and moved in a plane at right angles to the wind direction. Another characteristic of these windmills is that their rotation axes were usually manually or automatically aligned with the wind direction.

In the Mediterranean regions of Europe, the traditional windmills took the form of triangular canvas sails attached to radial arms. In northern Europe, such windmills were characterized by long rectangular sails consisting of either canvas sheets on lattice frameworks, so-called 'common sails', or 'shutter-type sails', which resembled venetian blinds. The shuttering arrangement gave a degree of control over starting, regulating and stopping the windmill according to wind strength.

In northern Europe there were two main forms of windmill. One was the less common 'post mill', in which the whole windmill was moved about a large upright post when the wind direction changed; the other was the more common 'tower mill' (Figure 8.10), in which the rotor and cap were supported by a relatively tall tower, usually of masonry. In the tower mill, only the cap (in combination with the rotor and its shaft) were moved in response to changes in wind direction. The sails turned fairly slowly and provided mechanical power.

At their zenith, before the Industrial Revolution, it is estimated that there were some 10 000 of these windmills in Britain (Golding, 1955) and they formed a familiar feature of the countryside.

As an indication of how numerous windmills were in the English countryside, during the Eastern Tour of his Rural Rides in the 1830s William Cobbett wrote:

> The windmills in the vicinage are so numerous that I counted, whilst standing in one place, no less than seventeen. They are all painted or washed white; the sails are black; it was a fine morning, the wind was brisk, and their twirling altogether added greatly to the beauty of the scene, which having the broad and beautiful arm of the sea on the one hand, and the fields and meadows, studded with farm-houses, on the other, appeared to me to be the most beautiful sight of the kind that I had ever beheld.
>
> (Cobbett, 1830)

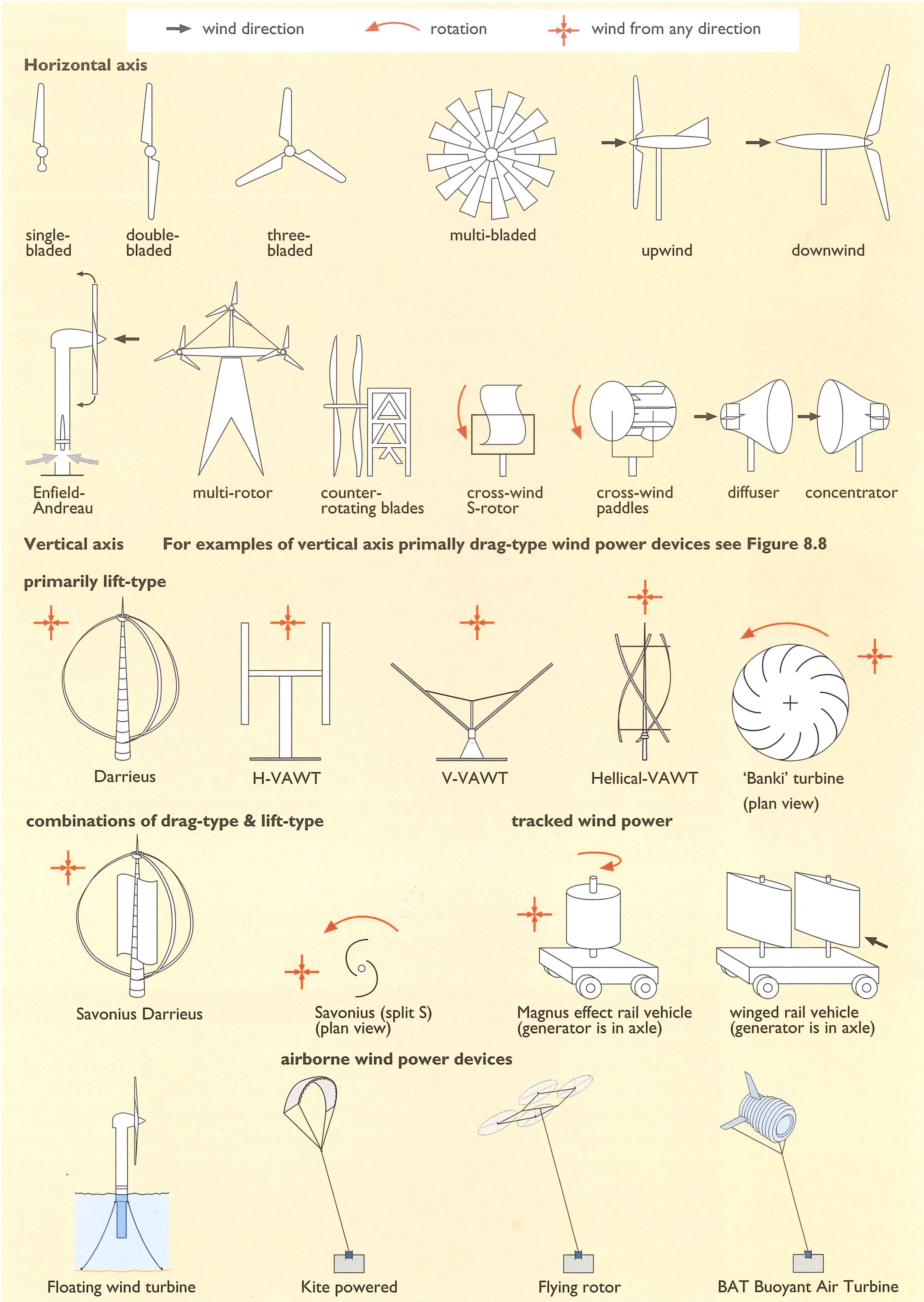

Figure 8.9 Some examples of the machines that have been proposed for wind energy conversion. (Source: partly based on Eldridge, 1975. For further information on these machines see Eldridge, 1975 and Golding, 1955). The figure includes mainly Horizontal axis and Vertical axis machines, but also includes a number of other types.

Figure 8.10 Traditional north European tower windmill

Wind turbine types

The variety of machines that has been devised or proposed to harness wind energy is considerable and includes many unusual devices. Figure 8.9 shows a small selection of the various types of machines that have been proposed over the years.

Most modern wind turbines come in one of two basic configurations: horizontal axis and vertical axis. Horizontal axis turbines are predominantly of the 'axial flow' type (i.e., the rotation axis is in line with the wind direction), whereas vertical axis turbines are generally of the 'cross flow' type (i.e., the rotation axis is perpendicular to the wind direction). They range in size from very small machines that produce a few tens or hundreds of watts to very large turbines producing as much as 8 MW. Larger turbines rated at 10 to 15 MW are now being considered and 20 MW designs and even 50 MW designs are being investigated.

Horizontal axis wind turbines

Figure 8.11 Multi-bladed wind pump

Horizontal axis wind turbines (HAWTs) generally have either two or three blades, but can have many more. Multi-bladed wind turbines have what appears to be virtually a solid disc covered by many solid blades (usually of slightly cambered sheet metal construction). They have been used since the nineteenth century for water pumping on farms (Figure 8.11). Appropriately for their application they produce high torque at low rotor speeds.

The term '**solidity**' is used to describe the fraction of the swept area that is solid. Wind turbines with large numbers of blades, such as these multi-bladed devices, have highly solid swept areas and are referred to as **high-solidity** wind turbines. Wind turbines with small numbers of narrow blades have a swept area that is largely void: only a very small fraction of the area appears to be 'solid' – such devices are referred to as **low-solidity** wind turbines. Multi-blade wind pumps have **high-solidity rotors** and modern electricity-generating wind turbines (with one, two or three blades) have **low-solidity rotors**.

Low-solidity devices work effectively at much higher rotational speeds making them attractive for electricity generation (Box 8.2 discusses the effect of blade number on turbine characteristics).

BOX 8.2 Effect of the number of blades

The speed of rotation of a wind turbine is usually measured in either revolutions per minute (rpm) or radians per second (rad s^{-1}). The **rotation speed** in revolutions per minute (rpm) is usually symbolized by N and the **angular velocity** in radians per second is usually symbolized by Ω. The relationship between the two is given by:

$$1\text{ rpm} = \frac{2\pi}{60}\text{ rad s}^{-1} = 0.10472\text{ rad s}^{-1}$$

A useful alternative measure of wind turbine rotor speed is **tip speed**, U, which is the **tangential velocity** of the rotor at the tip of the blades, measured in metres per second. It is the product of the angular velocity, Ω, of the rotor and the **tip radius**, R (in metres):

$$U = \Omega R$$

Alternatively, U can be defined as:

$$U = \frac{2\pi RN}{60}$$

By dividing the tip speed, U, by the **undisturbed wind velocity**, V_0, upstream of the rotor, we obtain a non-dimensional ratio known as the **tip speed ratio**, usually symbolized by λ. This ratio provides a useful measure against which aerodynamic efficiency can be plotted. The aerodynamic efficiency of a wind turbine is usually described as its **power coefficient** (effectively the ratio of power output from the turbine to the theoretical power in the wind). This quantity is symbolized by C_P and given as a fraction, such that 1 equates to 100% efficiency. When the power coefficient is plotted against tip speed ratio, such $C_P - \lambda$ curves provide an effective way to present the performance of a rotor and to compare wind turbines with differing characteristics.

A wind turbine of a particular design can operate over a range of tip speed ratios, but will usually operate with its best (maximum) efficiency at a particular tip speed ratio, i.e. when the velocity of its blade tips is a particular multiple of the wind velocity. This optimum tip speed ratio (λ_{opt}) is also commonly denoted as λ_{max} with the corresponding efficiency (i.e. power coefficient) being C_{Pmax}. The optimum tip speed ratio for a given wind turbine rotor will depend upon both the number of blades and the width of each blade.

In order to extract energy as efficiently as possible, the blades have to interact with as much as possible of the wind passing through the rotor's **swept area**. The blades of a high-solidity, multi-blade wind turbine interact with all the wind at very low tip speed ratios, whereas the blades of a low-solidity turbine have to travel much faster to 'virtually fill up' the swept area, in order to interact with all the wind passing through. If the tip speed ratio is too low, some of the wind travels through the rotor swept area without interacting with the blades; whereas if the tip speed ratio is too high, the turbine offers too much resistance to the wind, so that some of the wind goes around it. A two-bladed wind turbine rotor with each blade the same width as those of a three-bladed rotor will have an optimum tip speed ratio *one-third higher* than that of a three-bladed rotor. Optimum tip speed ratios for modern low-solidity wind turbines range between about 6 and 20.

In theory, the more blades a wind turbine rotor has, the more efficient it is. However, when there are large numbers of blades in a rotor, the flow becomes more disturbed, so that they aerodynamically interfere with each other. Thus high-solidity wind turbines tend to be less efficient overall than low-solidity turbines. Of low-solidity machines, three-bladed rotors tend to be the most energy efficient; two-bladed rotors are slightly less efficient and one-bladed rotors slightly less efficient still. Wind turbines with more blades can be generally expected to generate less aerodynamic noise as they operate at lower tip speeds (see Section 8.6) than wind turbines with fewer blades.

The mechanical power that a wind turbine extracts from the wind is the product of its angular velocity and the torque imparted by the wind. **Torque** is the moment about the centre of rotation due to the driving force imparted by the wind to the rotor blades. Torque is usually measured in newton metres (N m) (see Box 8.4). For a given amount of power, the *lower* the angular velocity the *higher* the torque; and conversely, the *higher* the angular velocity the *lower* the torque.

The pumps that are used with water pumping wind turbines require a high starting torque to function. Multi-bladed turbines are therefore generally


Figure 8.12 Two-bladed HAWT (WEG MS400 turbine)

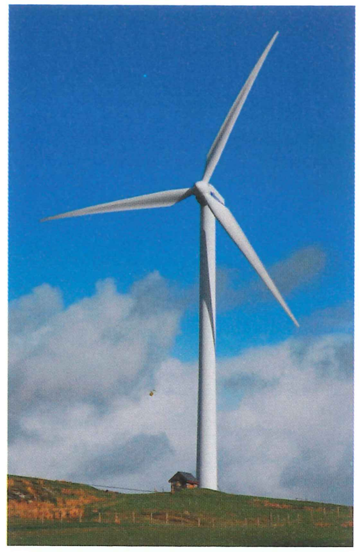
Figure 8.13 Three-bladed HAWT (Vestas V52 850 kW turbine)

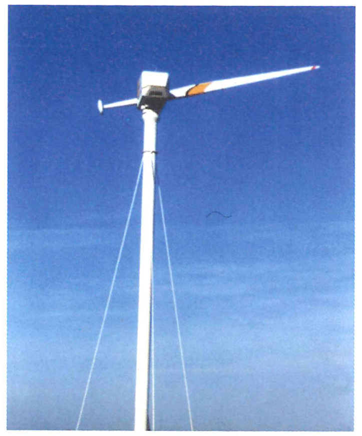
Figure 8.14 Single bladed HAWT (MBB 600 kW turbine)

used here because of their low tip speed ratios and resulting high torque characteristics.

Conventional electrical generators run at speeds many times greater than most wind turbine rotors so they generally require some form of gearing when used with wind turbines. Low-solidity wind turbines are better suited to electricity generation because they operate at high tip speed ratios and therefore do not require as high a gear ratio to match the speed of the rotor to that of the generator. In addition, many low-solidity small wind turbines (and even certain very large wind turbines) have avoided using gearboxes by using directly coupled low-speed multi-pole generators.

Modern *low-solidity* HAWT rotors evolved from traditional windmills and superficially resemble aircraft propellers. Wind turbines with such rotors are by far the most common design manufactured today. They have a clean streamlined appearance, due in part to their design being driven by aerodynamic considerations derived largely from developments in aircraft wing and propeller design. HAWT rotors generally have two or three wing-like blades (Figures 8.12 and 8.13). They are almost universally employed to generate electricity. Some experimental single bladed HAWTs have also been produced (Figure 8.14) and continue to be researched. Three blades are the most common, though two and single bladed rotors may be beneficial in very large rotors being research for offshore HAWTs.

Vertical axis wind turbines

Vertical axis wind turbines (VAWTs) that employ aerofoil type blades, unlike their horizontal axis counterparts, can harness winds from any direction without the need to reposition the rotor when the wind direction changes. However, despite this advantage, they have found little commercial success to date, in part because – unlike HAWTs – they have not been able to benefit from the experience curve, and in part it may be due to issues with power quality, cyclic loads on the tower systems and the lower efficiency of some VAWT designs. At the micro/small scale, they tend to have lower aerodynamic efficiency and tend to require more expensive rotors compared to micro/small HAWTs. A technical description of how aerofoil-based VAWTs operate is given in Section 8.4.

The modern aerofoil-based VAWT evolved from the ideas of the French engineer, Georges Darrieus, whose name is used to describe one of the VAWTs that he invented in 1925 – such devices were independently reinvented in Canada by South and Rangi at the National Aeronautical Establishment of the National Research Council in the 1960s (South and Rangi, 1972). This device, which resembles a large eggbeater, has curved blades (each with a symmetrical aerofoil cross-section) the ends of which are attached to the top and bottom of a vertical shaft (see Figure 8.15). Several hundred were manufactured in the USA and installed in wind farms in California in the 1980s. A small number were produced in Canada, including 'Eole', the largest VAWT yet built, a 100 m tall 60 m diameter turbine. Eole operated for six years from 1988 in Quebec and achieved a 94% availability (see Figure 8.15(b)).

These Darrieus VAWTs were guyed structures, which added complexity and limited their height, though a Dutch 15 m diameter 100 kW Darrieus VAWT on a cantilevered tower was built in the 1980s and a new design of Darrieus VAWT, mounted on a free-standing cantilevered tower that avoids the difficulties of guys, is under development in New Mexico (VPM, 2017). There was also a floating enhanced Darrieus VAWT design under development (FWC, 2017). Sandia Laboratories carried out a retrospective review of VAWTs and are also researching the potential for large Darrieus VAWTs for offshore applications.

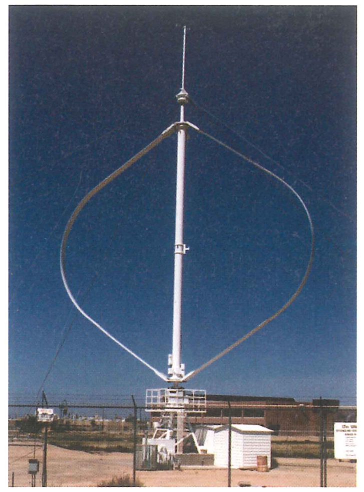
(a)


(b)

Figure 8.15 (a) Seventeen metre diameter Darrieus-type VAWT at Sandia National Laboratories, New Mexico.
(b) Sixty metre diameter Eole VAWT in Quebec, Canada

The blades of a Darrieus VAWT take the form of a 'troposkein' (the curved, arch-like shape taken by a spinning skipping rope). This shape is a structurally efficient one, well suited to coping with the relatively high centrifugal forces acting on VAWT blades. However, they can be difficult to manufacture, transport and install, though the advent of modern composites and manufacturing methods may help to address some of the difficulties. In order to overcome these problems, straight-bladed VAWTs have been developed: these include the 'H'-type vertical axis wind turbine (H-VAWT) and the 'V'-type vertical axis wind turbine (V-VAWT). Interestingly Sandia Laboratories in their retrospective review of VAWTs concluded 'that VAWTs do have significant advantages over HAWTs in offshore applications. ... Their primary disadvantage remains the longer blade length required by the full Darrieus VAWT configurations. ... Both the 'H' and the 'Y' (e.g. the 'V') configurations offer potential for variable, cost effective designs.' (Sutherland et al., 2012).

The H-VAWT (Figure 8.16) consists of a tower (which may house a vertical shaft), capped by a hub to which is attached two or more horizontal cross arms that support the straight, upright, aerofoil blades. In the UK, this type of turbine was developed by VAWT Ltd which built 125 kW and 500 kW prototypes at Carmarthen Bay and a 100 kW turbine on the Isles of Scilly in the 1980s. There continues to be interest in H-VAWTs both at small scale and for large offshore applications (VertAx, 2017).

The V-VAWT consists of straight aerofoil blades attached at one end to a hub on a vertical shaft and inclined in the form of a letter 'V'. Its main features include a shorter tower, shorter shaft compared to the Darrieus VAWT, ground/water level-mounted generator options, ground/water level blade installation via hinged blades and the ability to self start without needing complex variable pitch blades or the electrical starting required by other types of VAWTs. Experimental prototypes were tested at the Open University (Figure 8.17(a)) as was the *Sycamore Rotor*, a single bladed version. New generation *V2 turbine* variants (Figure 8.17(b)) and other novel derivative configurations suited to very large scale and offshore fixed/floating applications are being researched by the author.


Figure 8.16 500 kW 'h'-type VAWT at Carmarthen Bay, Wales

At the present time, VAWTs are not generally economically competitive with HAWTs. However, they continue to attract research as they should, in principle, offer significant advantages over HAWTs in terms of blade loading and fatigue, if they can be built in very large sizes (such as are becoming desired for use in offshore applications). Whilst VAWTs are subject to wind-induced cyclic loads (which do not progressively increase with increasing size of turbine) they are not subject to the major gravitational cyclic loadings (which do progressively increase with rotor diameter) that large diameter HAWTs experience. As the Canadian Eole demonstrated in the 1980s/90s, large VAWTs can be operated with very high reliability.

More recent variants in aerofoil-based vertical axis wind turbines are VAWTs with helically shaped blades. These were first advocated in the 1990s by the Swedish engineer Olle Ljungstrom and additionally by US engineer Alexander Gorlov. Gorlov also suggested such turbines could be used in hydro and, as discussed in Chapter 7, tidal current applications (Gorlov, 1998). Stimulated by perceived concerns about cyclic torque (due to the cyclic variation in the position of a VAWTs blade, relative to the wind direction – see Section 8.4), in the 1990s Ljungstrom produced designs of Darrieus VAWTs that employed helically shaped blades. A number of more recent designs have employed such blades. In practice, however, simply employing three blades should usually be sufficient to even out the torque variation for VAWTs, without the extra complexity and high cost of manufacturing helical blades (Musgrove, 1990, cited in Freris, 1990).

As was mentioned above, most types of aerofoil-based VAWTs are not able to self-start without some extra mechanism (as they are generally unable to produce sufficient aerodynamic starting torque). Examples of such additions are drag-driven 'vertical axis starter rotors' (which can reduce aerodynamic efficiency), complex variable pitch blades, or some form of electrical starting mechanism. Electrically assisted starting is not a major issue for the medium/large scale VAWTs employed in wind farms, but it is a major shortcoming for small/micro scale VAWTs, especially for off-grid applications or on relatively low wind speed sites, when electrically started VAWTs can consume large amounts of electricity, thus greatly reducing their net productivity (Day et al., 2010).

(a)

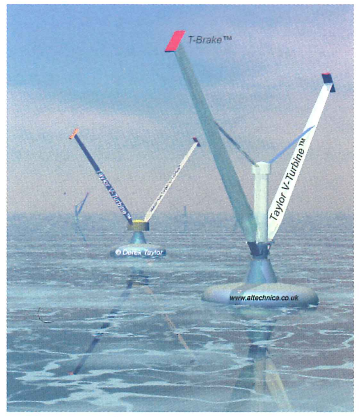

(b)

Figure 8.17 (a) V-VAWT prototype developed and tested at the Open University in Milton Keynes in the 1980s (b) multi megawatt scale V-Turbine concept in offshore configuration

8.4 Aerodynamics of wind turbines

Aerodynamic forces

When a force is transferred by a moving solid object to another solid object, the second object will generally move in either the same direction or in a direction at a small angle (less than 90 degrees) to the direction of motion of the first object, unless subjected to another force. However, the method by which forces are transferred from a fluid to a solid object is very different.

Wind turbines are operating in an unconstrained fluid, in this case air. To understand how they work, two terms from the field of aerodynamics will be introduced. These are 'drag' and 'lift'.

An object in an air stream experiences a force that is imparted from the air stream to that object (Figure 8.18). We can consider this force to be equivalent to two component forces acting in perpendicular directions, known as the *drag force* and the *lift force*. The magnitude of these drag and lift forces depends on the shape of the object, its orientation to the direction of the air stream, and the velocity of the air stream.

The **drag force** is the component that is in line with the direction of the air stream. A flat plate in an air stream, for example, experiences maximum drag forces when the direction of the air flow is perpendicular (that is, at right angles) to the flat side of the plate; when the direction of the air stream is in line with the flat side of the plate, the drag forces are at a minimum.

Traditional vertical axis windmills and undershot water wheels (see Chapter 6) are driven largely by drag forces.

Objects designed to minimize the drag forces experienced in an air stream are described as streamlined, because the lines of flow around them follow smooth, stream-like lines. Examples of streamlined shapes are teardrops, the shapes of fish such as sharks and trout, and aeroplane wing sections (aerofoils) (Figure 8.19).

The **lift force** is the component that is at right angles to the direction of the air stream. It is termed 'lift' force because it is the force that enables aeroplanes to *lift* off the ground and fly, though in other applications it may induce a *sideward* (as in a sailboat) or *downward* force (as in the downforce aerofoil used in some racing cars). Lift forces acting on a flat plate are smallest when the direction of the air stream is at a zero angle to the flat surface of the plate. At small angles relative to the direction of the air stream – that is, when the so-called *angle of attack* (see below for more detail) is small – a low pressure region is created on the 'downstream' (or 'leeward') side of the plate as a result of an increase in the air velocity on that side (Figures 8.20 and 8.21 show this effect on aerofoil sections).

In this situation, there is a direct relationship between air speed and pressure: the faster the airflow, the lower the pressure (i.e. the greater the 'suction effect'). This phenomenon is known as the **Bernoulli effect** after Daniel Bernoulli, the Swiss mathematician who first explained it. The lift force thus acts as a 'suction' or 'pulling' force on the object, in a direction at right angles to the airflow.

As well as enabling aeroplanes and gliders to fly, it is the lift force that propels modern sailing yachts, and supports and propels helicopters. Lift is also the principal force that drives a modern wind turbine rotor and thus allows it to produce power.

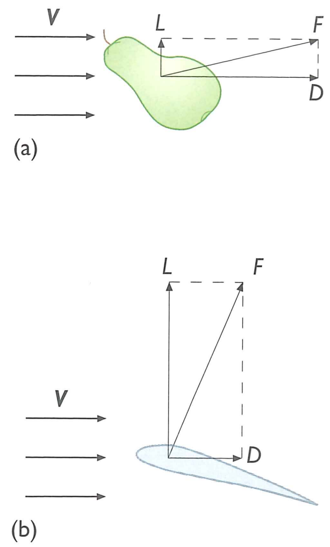

Figure 8.18 (a) and (b) An object in an air stream is subjected to a force, F, from the air stream. This is composed of two component forces: the drag force, D, acting in line with the direction of air flow and the lift force, L, acting at 90° to the direction of air flow

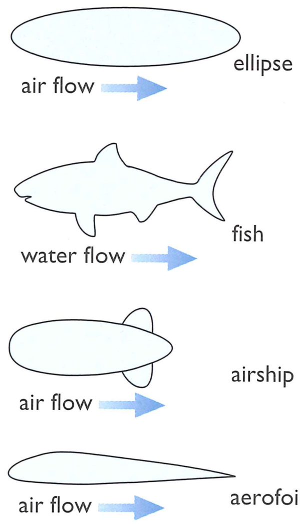

Figure 8.19 Some examples of streamlined shapes

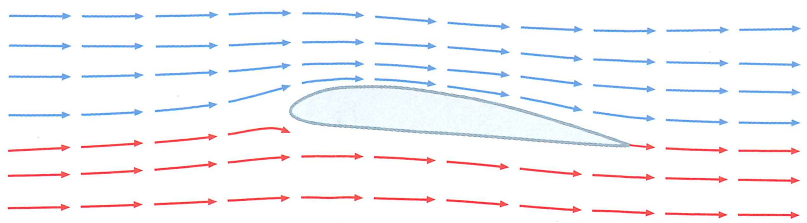

Figure 8.20 Streamlined flow around an aerofoil section

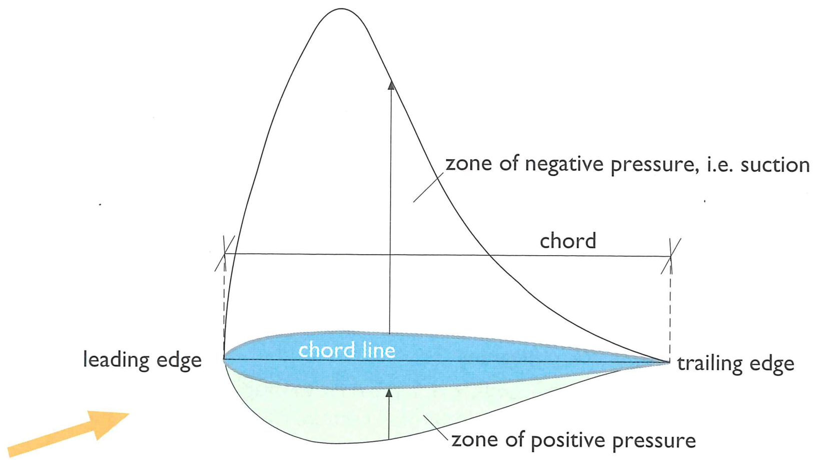

Figure 8.21 Zones of low and high pressure around an aerofoil section in an air

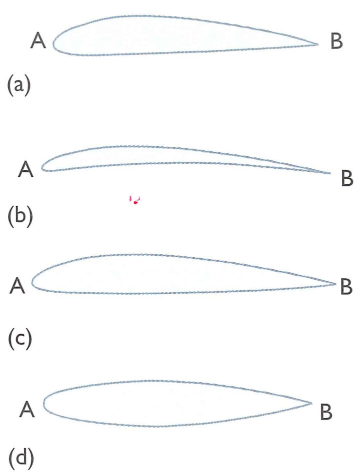

Figure 8.22 Types of aerofoil section: (a), (b) and (c) are various forms of asymmetrical aerofoil section and (d) is a symmetrical aerofoil section

Aerofoils

Arching or cambering a flat plate will cause it to induce higher lift forces for a given angle of attack, but the use of so-called **aerofoil sections** is even more effective. There are two main types of aerofoil section that are conventionally distinguished: asymmetrical and symmetrical (Figure 8.22). Both have a markedly convex upper surface, a rounded end called the 'leading edge' (which faces the direction from which the air stream is coming), and a pointed or sharp end called the 'trailing edge'. It is the shape of the 'under surface' or high pressure side of the sections that identifies the type. Asymmetrical aerofoils are optimized to produce most lift when the underside of the aerofoil is closest to the direction from which the air is flowing. Symmetrical aerofoils are able to induce lift equally well (although in opposite directions) when the air flow is approaching from either side of the **chord line** (the 'length', from the tip of its leading edge to the tip of its trailing edge, of an aerofoil section).

The angle which an aerofoil (or flat or cambered plate profile) makes with the direction of an airflow, measured against a reference line (usually the chord line of the aerofoil), is called the **angle of attack** α (alpha) (Figure 8.23). When airflow is directed towards the underside of the aerofoil, the angle of attack is usually referred to as positive.

When employed as a wing profile, asymmetrical aerofoil sections will, subject to a net incident airflow velocity (in aircraft this is due to forward flight), tend to accelerate the airflow over the more convex 'upper' surface. The high air speed thus induced results in a large reduction in pressure over

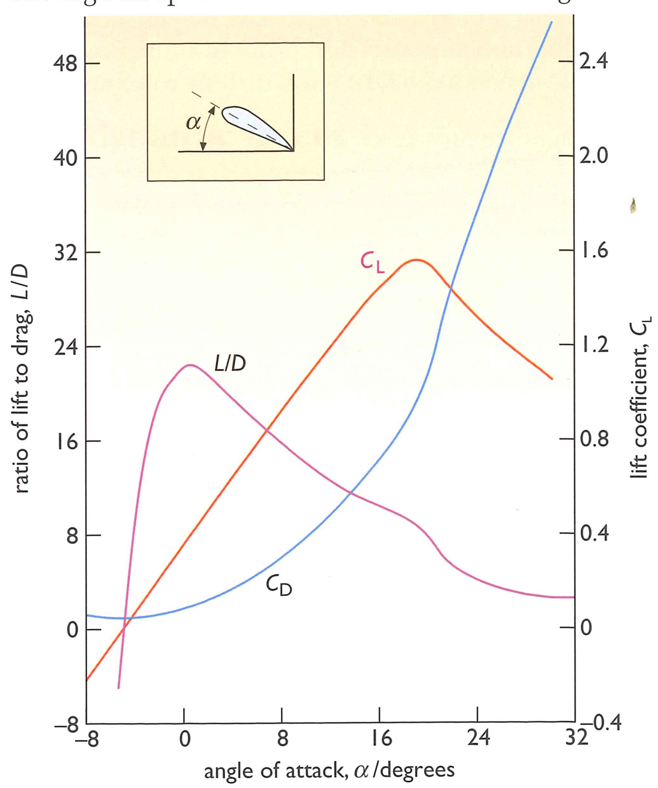

Figure 8.23 Lift coefficient, C_L, drag coefficient, C_d, and lift to drag ratio (L/D) versus angle of attack, α (shown inset), for a Clark Y aerofoil section. The region just to the right of the peak in the C_L curve corresponds to the angle of attack at which stall occurs

the upper surface relative to the lower surface. This results in a 'suction' effect which 'lifts' the aerofoil-shaped wing, although it should be noted that this lift can only be sustained if the airflow leaves the aerofoil at the downstream edge (known as the trailing edge) in a smooth manner that prevents the high pressure air recirculating around the trailing edge and cancelling out the reduced pressure. The strength of the lift force induced by an aerofoil section is well demonstrated by its ability to support the entire mass of a large aircraft such as the Airbus A380.

The lift and drag characteristics of many different aerofoil shapes, for a range of angles of attack, have been determined by measurements taken in wind tunnel tests, and catalogued (e.g. in Abbott and von Doenhoff, 1958). The lift and drag characteristics measured at each angle of attack can be described using non-dimensional **lift** and **drag coefficients** (C_L and C_D) or as **lift to drag ratios** (C_L/C_D). These are defined in Box 8.3.

BOX 8.3 Aerofoil sections and lift and drag coefficients

Note that the chord of an aerofoil section is also the same as the *width* of the blade in a wind turbine at a given position along the blade.

Drag coefficient (C_D)

The drag coefficient of an aerofoil is given by the following expression:

$$C_D = \frac{D}{0.5\rho V^2 A_b}$$

where:

D is the drag force in newtons (N)

ρ is the air density in kilograms per cubic metre (kg m^{-3})

V is the velocity of the air approaching the aerofoil in metres per second (m s^{-1})

A_b is the blade area (i.e. chord × length) in square metres (m^2).

In the case of a blade element, the area is equal to the mean chord × length of the blade element.

Lift coefficient (C_L)

The lift coefficient of an aerofoil is given by the following expression:

$$C_L = \frac{L}{0.5\rho V^2 A_b}$$

where L is the lift force in newtons.

The lift and drag coefficients of an aerofoil can be measured in a wind tunnel at different angles of attack and wind velocities. The results of such measurements can be presented in either tabular or graphical form as in Figure 8.23.

Each aerofoil has an angle of attack at which the lift to drag ratio (C_L/C_D) is at a maximum. This angle of attack results in the maximum force and is thus the most efficient setting of the blades of a HAWT. Consequently, plots of this ratio against angle of attack can be useful to turbine designers (Figure 8.23).

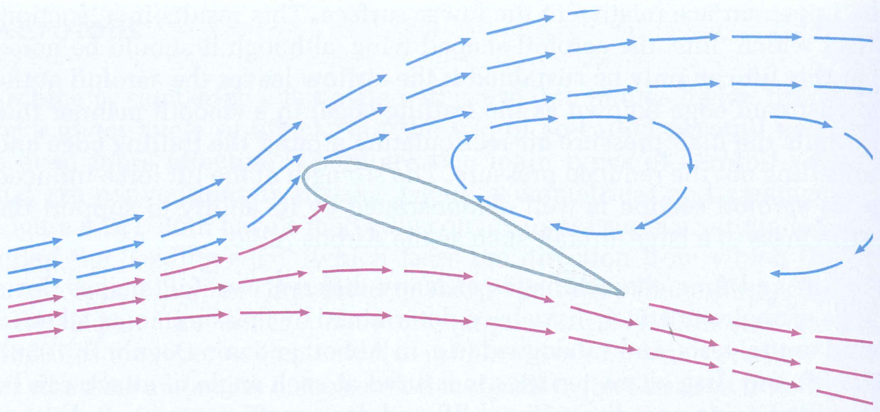

Figure 8.24 Aerofoil section in stall

Another important characteristic relationship of an aerofoil is its **stall angle**. This is the angle of attack at which the aerofoil exhibits stall behaviour. Stall occurs when the flow suddenly leaves the suction side of the aerofoil (when the angle of attack becomes too large), resulting in a dramatic loss in lift and an increase in drag (Figures 8.23 and 8.24). When this happens during the flight of an aeroplane, it can be extremely dangerous unless the pilot can make the plane recover. One of the methods used by wind turbines to limit the power extracted by the rotor in high winds takes advantage of this phenomenon; such turbines are known as stall regulated (see below for more details).

Aerofoils can also now be designed with the aid of specially developed software, and new aerofoils are being designed and optimized to be more efficient in the aerodynamic conditions experienced by wind turbines. Examples of wind turbine specific aerofoils include the DU airfoils (Rooij and Timmer, 2004) and NREL airfoils (Tangler and Somers, 1995). Figure 8.23 shows typical lift and drag coefficients, and lift to drag ratios, for one aerofoil section. Knowledge of these coefficients is essential when selecting appropriate aerofoil sections in wind turbine blade design. The lift and drag forces experienced are both proportional to the energy in the wind.

Relative wind velocity

When a wind turbine is stationary, the direction of the wind as 'seen' from a wind turbine blade is the same as the undisturbed wind direction. However, once the blade is moving, the direction from which it 'sees' the wind approaching effectively changes in proportion to the blade's velocity. (In the case of a moving vertical axis wind turbine blade, the direction from which the blade 'sees' the wind is additionally affected by its position during its rotation cycle – see Figure 8.27). Two-dimensional **vectors** are used to represent this effect graphically. A two-dimensional vector is a quantity that has both magnitude and direction. A velocity vector can be represented graphically in the form of an arrow, the length of which is proportional to speed, and the angular position of which indicates the direction of flow.

The wind as seen from a point on a moving blade is known as the **relative wind**, and its velocity is known as the **relative wind velocity** (usually

symbolized by W). This is a vector which is the resultant (i.e. the vector sum) of the **wind velocity at the rotor**, V_1 (i.e. the **undisturbed wind velocity vector**, V_0, reduced by a factor known as the axial interference factor) and the tangential velocity vector of the blade at that point on the blade, $\boldsymbol{u}$ (see Box 8.4). Note that the tangential velocity, measured in metres per second (m s^{-1}), is distinct from the angular velocity, which is measured in radians per second or in revolutions per minute (Box 8.2).

The angle from which the point on the moving blade sees the relative wind is known as the **relative wind angle** (usually symbolized by ϕ) and is measured from the tangential velocity vector, $\boldsymbol{u}$. The **blade pitch angle**, β, at this point on the blade is the relative wind angle minus the angle of attack, α, at that point on the blade (see Box 8.4).

Harnessing aerodynamic forces

Modern horizontal and vertical axis wind turbines make use of the aerodynamic forces generated by aerofoils in order to extract power from the wind, but each harnesses these forces in a different way.

In the case of a HAWT with fixed-pitch blades with its rotor axis assumed to be in constant alignment with the undisturbed wind direction, for a given wind speed and constant rotation speed, the angle of attack at a given position on the rotor blade *stays constant throughout its rotation cycle* (Box 8.4).

BOX 8.4 **HAWT rotor blades wind forces and velocities**

Figure 8.25 shows a section through a moving rotor blade of a HAWT. Also shown is a vector diagram of the forces and velocities at a position along the blade at an instant in time.

Because the blade is in motion, the direction from which the blade 'sees' the relative wind velocity, W, is the resultant of the tangential velocity, $\boldsymbol{u}$, of the blade at that position and the wind velocity at the rotor, V_1. Note that in this diagram, the direction of $\boldsymbol{u}$ is shown in the opposite direction to the direction of motion of the rotating blade, in the same manner that a flag on a motor boat moving in calm weather points to the stern of the boat, showing the air to be 'flowing' from the opposite direction to the boat's forward motion.

The wind velocity at the rotor, V_1, is the undisturbed wind velocity upstream of the rotor, V_0, reduced by a factor that takes account of the wind being slowed down as a result of power extraction. This factor is often referred to as the **axial interference factor**, and is represented by a.

The tangential velocity, $\boldsymbol{u}$, (in metres per second) at a point along the blade is the product of the angular velocity, Ω (in radians per second) of the rotor and the local radius, r, (in metres), at that point, that is:

$$u = \Omega r \quad (3)$$

Albert Betz showed in 1928 that the maximum fraction of the power in the wind that can theoretically be extracted is 16/27 (59.3%). This occurs when the undisturbed wind velocity is reduced by one-third, in other words, when the axial interference factor, a, is equal to one-third. The value of 59.3% is often referred to as the **Betz limit**.

The relative wind angle, ϕ, is the angle that the relative wind makes with the blade (at a particular point with local radius, r, along the blade) and is measured from the plane of rotation. (Note: if it were not for the fact that the wind is slowed down as a result of the wind turbine extracting energy – in other words if V_0 was not reduced to V_1 at the rotor – the tip speed ratio would be equal to the reciprocal of the tangent of the relative wind angle at the blade.) The angle of attack, α, at this point on the blade can be measured against the relative wind angle, ϕ. The blade pitch angle (usually represented by β) is then *equal* to the relative wind angle *minus* the angle of attack. Since the rotor is constrained

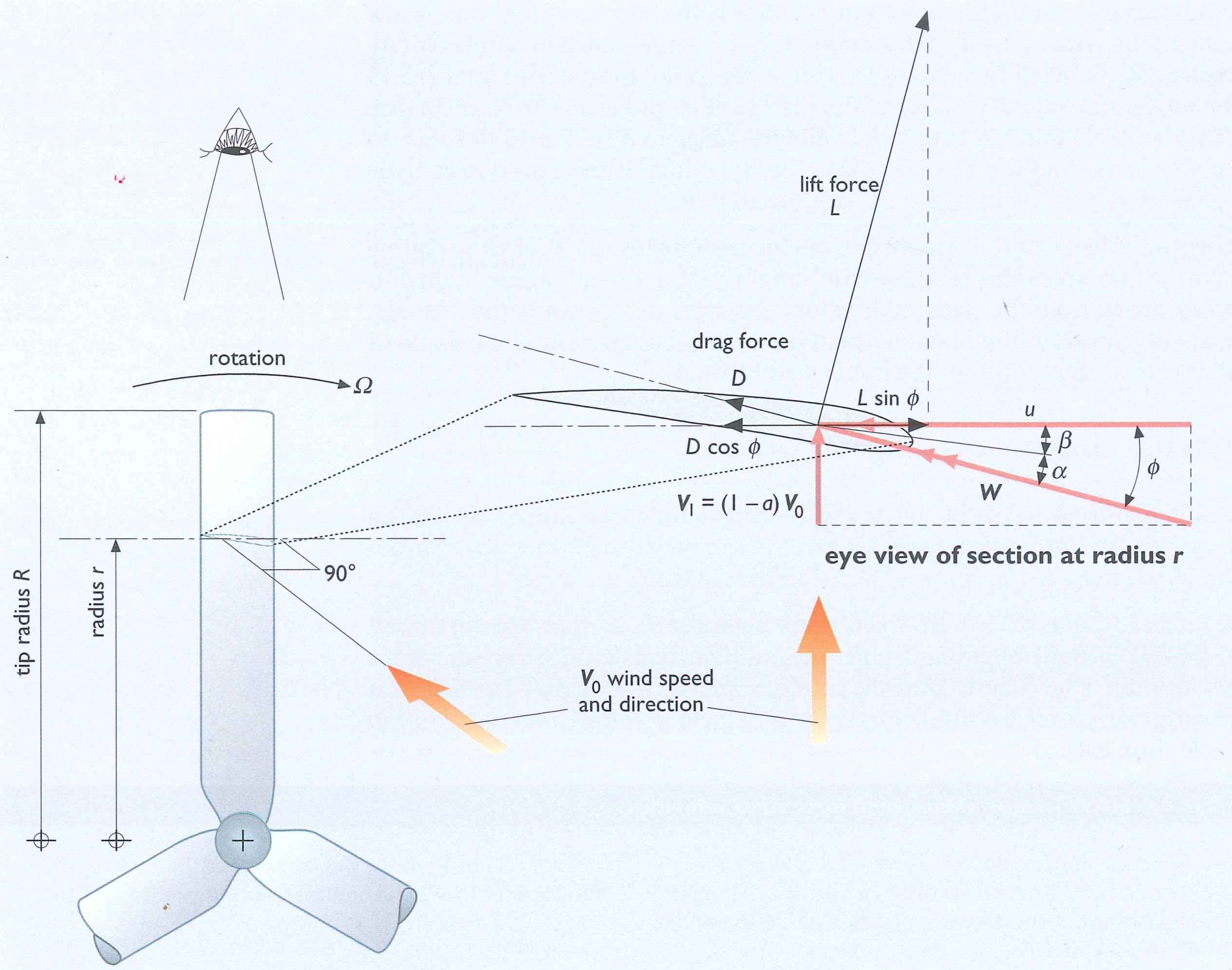

Figure 8.25 Vector diagram showing a section through a moving HAWT rotor blade. Notice that the drag force, D, at the point shown is acting in line with the direction of the relative wind, W, and the lift force, L, is acting at 90° to it

to rotate in a plane at right angles to the undisturbed wind, the driving force at a given point on the blade is that component of the aerofoil lift force that *acts in the plane of rotation*. This is given by the product of the lift force, L, and the sine of the relative wind angle, ϕ (that is, $L \sin \phi$). The component of the drag force in the rotor plane at this point is the product of the drag force, D, and the cosine of the relative wind angle, ϕ (that is, $D \cos \phi$).

The torque, q (that is, the moment about the centre of rotation of the rotor in the plane of the rotor), in newton metres (N m) at this point on the blade is equal to the *product* of the *net driving force in the plane of rotation* (that is, the component of lift force in the plane of rotation minus the component of the drag force in the rotor plane) and the local radius, r. The total torque, Q, acting on the rotor can be calculated by summing the torque at all points along the length of the blade and multiplying by the *number* of blades. The power from the rotor is the *product* of the total torque, Q and the rotor's angular velocity, Ω.

Why are rotor blades twisted?

The magnitude and direction of the relative wind angle, ϕ, varies along the length of the blade according to the local radius, r. Equation (3) shows that the tangential velocity varies with radius, so as the tangential speed *decreases* towards the hub, the relative wind angle, ϕ, *progressively increases* (see Figure 8.26). A HAWT rotor designed for optimum performance will have a tapered blade, and to have a constant angle of attack along its length (assuming the same aerofoil section is used throughout its length), it will have to have a built-in twist. The amount of twist will vary (as the relative wind angle varies) progressively from tip to root. Figure 8.26 demonstrates the progressive twist of such a HAWT rotor blade. Most manufacturers of HAWT blades use tapered and twisted blades, although it

is possible to build functional HAWT rotor blades that are not twisted. These are cheaper, but less efficient and how well they function depends in part on both the aerofoil characteristics and the overall blade pitch angle.

Blade pitch

As well as the blade pitch angle defined above, the term **blade pitch** also refers to the whole blade's angular position about the blade's longitudinal axis (also known as the pitch axis) such that in the case of a **variable pitch** rotor blade, the whole blade is able to be rotated about its pitch axis. In most cases all of the blades of a variable pitch HAWT rotor change pitch at the same time in order to:

- optimise the turbine's power production across a range of wind speeds (in order to maintain the angle of attack at or near to the optimal angle across a range of wind speeds)
- reduce its output at high wind speeds
- to stop the rotor during very high wind speeds or to 'park' the rotor (such that the blade pitch is in its 'feathered' position, e.g. each blade pitch is at or near 90 degrees, relative to the plane of rotation), when it is necessary to prevent the rotor from operating for any reason.

In the case of a **fixed pitch** rotor the blade pitch angle remains unchanged, which makes them less productive and less controllable. Most large wind turbines employ variable pitch blades, but most micro wind turbines and small wind turbines and some medium-scale wind turbines use fixed pitch blades.

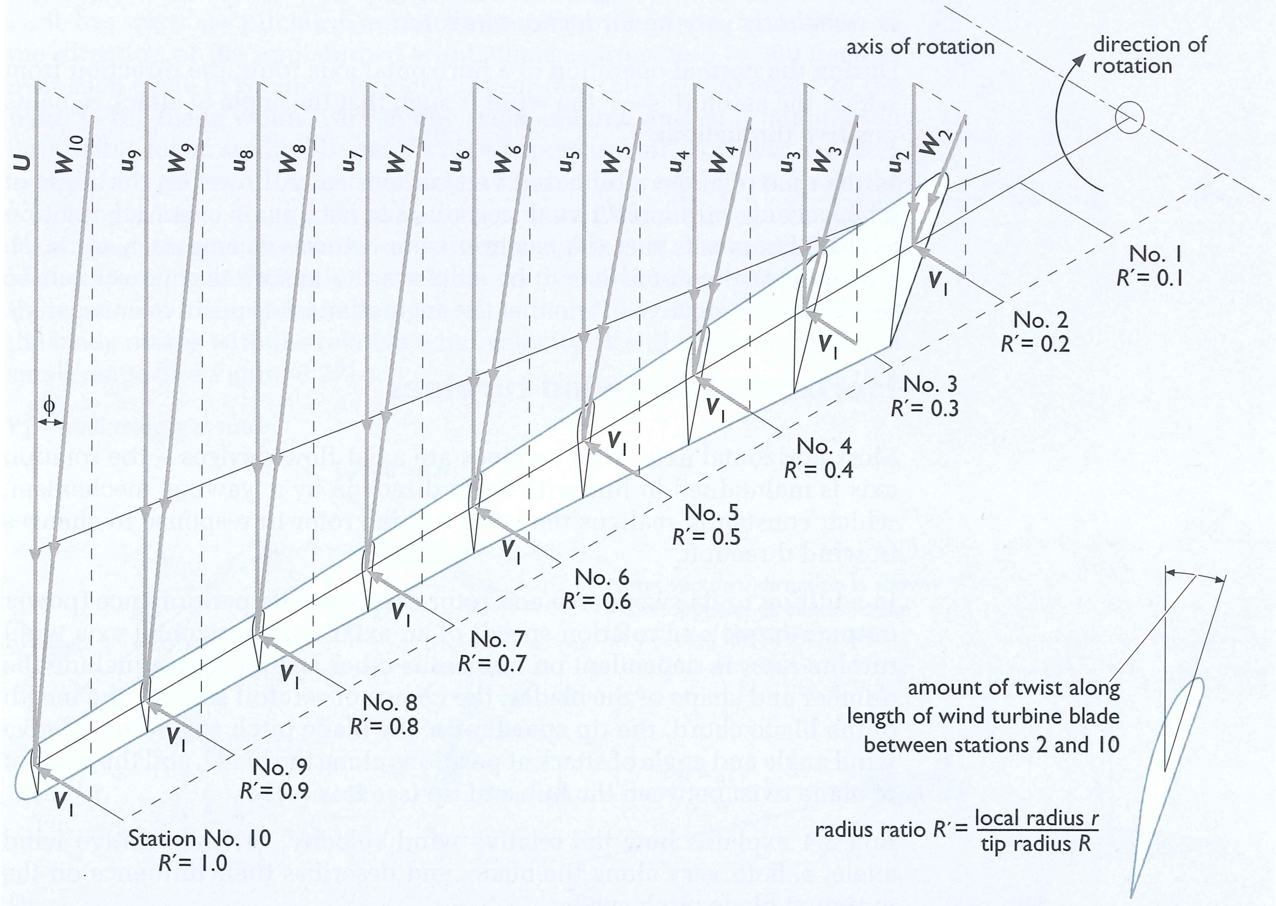

Figure 8.26 Three-dimensional view of an optimally tapered and twisted HAWT rotor blade design (the blade is shown in a horizontal position and moving through the upward part of its cycle about its axis of rotation). The figure shows how the relative wind angle, ϕ, changes along the blade span (length). Note that the blade aerofoil section and the angle of attack are assumed to be constant along the length of the blade. The diagram (lower right) of the view along the blade indicating the amount of built-in twist along the length of the blade shows the blade cross-section at station 2: the cross section of the blade at station 10 has been omitted for clarity

8.5 Power and energy from wind turbines

How much power does a wind turbine produce?

The power output of a wind turbine varies with wind speed: every turbine has a characteristic wind speed–power curve, often simply called the **power curve**. The shape of a wind speed–power curve is influenced by the:

- rotor swept area
- choice of aerofoil
- number of blades
- blade shape
- optimum tip speed ratio
- speed of rotation
- cut-in wind speed (the wind speed at which a turbine begins to generate power)
- rated wind speed (the wind speed at which a turbine generates its rated power)
- shut-down or cut-out wind speed (the wind speed at which a turbine is shut down and stops generating – also known as the furling wind speed)
- aerodynamic efficiency (power coefficient)
- gearing efficiency, and
- generator efficiency.

An example of such a curve is shown in Figure 8.28.

Figure 8.28 Typical wind turbine wind speed–power curve

How much energy will a wind turbine produce?

The energy that a wind turbine will produce depends on both its wind speed–power curve and the **wind speed frequency distribution** at the site. The latter is essentially a graph or histogram showing the number of hours for which the wind blows at different wind speeds during a given period of time. Figure 8.29 shows a typical wind speed frequency distribution.

For each incremental wind speed within the operating range of the turbine (that is, between the cut-in wind speed and the shut-down wind speed), the energy produced at that wind speed can be obtained by multiplying the number of hours of its duration by the corresponding turbine power at this wind speed (given by the turbine's wind speed–power curve). This data can then be used to plot a **wind energy distribution** such as that shown in Figure 8.30. The total energy produced in a given period is then calculated by summing the energy produced at all the wind speeds within the operating range of the turbine.

The best way to determine the wind speed distribution at a site is to carry out wind speed measurements with equipment that records the number of hours for which the wind speed lies within each given 1 m s^{-1} wide speed band, e.g. 0–1 m s^{-1}, 1–2 m s^{-1}, 2–3 m s^{-1}, etc.

The longer the period over which measurements are taken, the more accurate is the estimate of the wind speed frequency distribution. As the power in the wind is proportional to the cube of the wind velocity – see Equation (2) – a small error in estimating the wind speeds can produce a large error in the estimate of the energy yield.

Additional factors that affect the total energy generated include transmission losses and the availability of the turbine. **Availability** is an indication of the reliability of the turbine installation and is the fraction or percentage

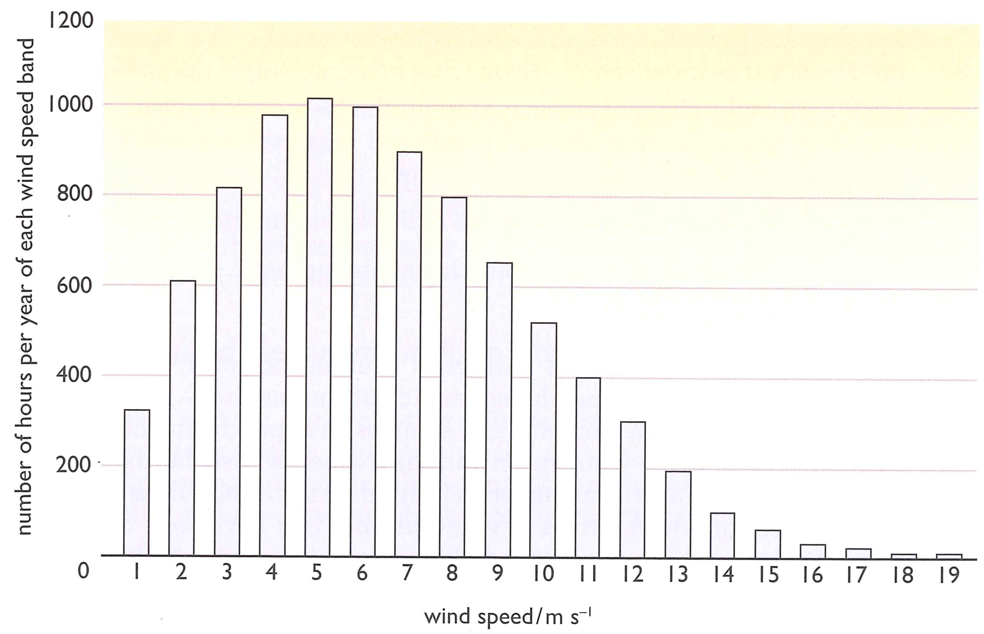

Figure 8.29 A wind speed frequency distribution for a typical site

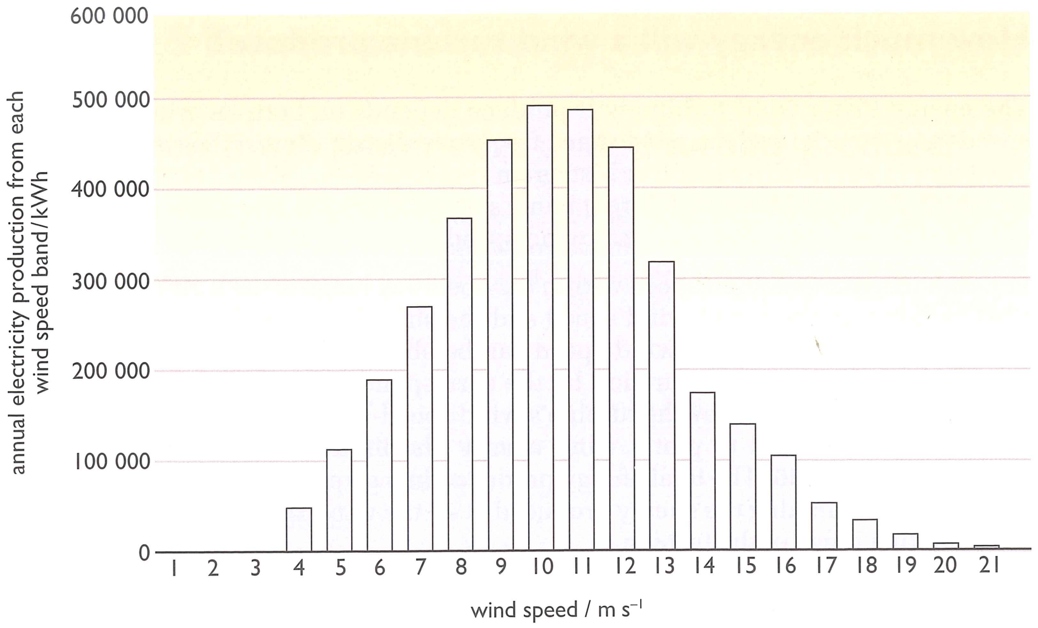

Figure 8.30 Wind energy distribution for the same site as in Figure 8.29, showing energy produced at this site by a wind turbine with the wind speed–power curve shown in Figure 8.28

of a given period of time for which a wind turbine is available to generate, when the wind is blowing within the turbine's operating range. Current commercial wind turbines typically have annual availabilities in excess of 90%, many have operated at over 95% and some are achieving 98%.

If the mean annual wind speed at a site is known, or can be estimated, the following formula (Beurskens and Jensen, 2001) can be used to make a rough *initial estimate* of the electricity production (in kilowatt-hours per year) from a number of wind turbines:

Annual electricity production $= K\, V_m^3\ A_t\ T$

where:

$K = 3.2$ and is a factor based on typical turbine performance characteristics and an approximate relationship between mean wind speed and wind speed frequency distribution (see below)

V_m is the annual mean wind speed at the site in metres per second

A_t is the swept area of the turbine in square metres

T is the number of turbines.

This formula should be used with great caution, however, because it is based on an average of the characteristics of the medium- to large-scale wind turbines currently available and assumes an approximate relationship between annual mean wind speed and the frequency distribution of wind speeds that may not be accurate for an individual site. It also does not allow for the different power curves of wind turbines that have been optimized either for low or high wind speed sites. The K factor of 3.2 given above assumes a well designed turbine suited to its site (Beurskens and Jensen, 2001), but it should not be used with small-scale wind turbines as their performance varies greatly and they are more likely to be located at sites with lower annual mean wind speeds and potentially in suburban and urban areas.

For a small wind turbine (less than 200 m^2 swept area) estimates of potential electricity production can be derived if the supplier provides a British Wind Energy Association Reference Annual Energy (RAE) value (BWEA, 2008) or an American Wind Energy Association Rated Annual Energy (RAE) value together with an AEP (Annual Energy Production) curve (AWEA, 2009). However there will still be a high level of uncertainty in urban areas. Knowing the IEC 61400 wind speed class that the turbine has been tested for also helps to estimate energy production.

Estimating the wind speed characteristics of a site

It is expensive to carry out detailed measurements at a site and wind speed measurements are often not carried out for small wind turbine installations. However the use of remote sensing methods such as SODAR (SOnic Detection And Ranging) and Doppler LIDAR (LIght Detection And Ranging) makes it feasible to monitor wind speeds without the need for tall towers. In addition, lower cost instrumentation is becoming available for monitoring small wind turbine sites.

It is preferable to record the wind speed and direction as close as possible to the proposed site for at least a year. However this will only give information for a particular time period, and weather patterns change. In order to ascertain the longer term wind speed characteristics, it is useful to correlate the measured data with data measured at one or more nearby meteorological stations or other wind recording sites. Then by statistical analysis of the two data sets, and extrapolating over the long-term data from the meteorological station, an estimate of the longer term wind speed characteristics at the site can be made. This technique is referred to as the **Measure–Correlate–Predict** or **MCP** method.

There are a number of different ways of implementing the MCP methodology all based on different statistical analysis techniques (Rogers et al, 2005, 2006a). These methods are embedded into different software packages, but their application requires careful judgement – consistency in the use of the methods is important and more than one algorithm should be employed in order to avoid bias.

If it is not possible to carry out wind speed and direction measurements at a proposed site, or where a preliminary analysis is required prior to installing instrumentation, there are a number of techniques that can be employed to give an approximate estimate of the wind speed characteristics of a site.

Using wind speed measurements from a nearby location

This involves making use of existing wind speed measurements from one or more locations nearby and deriving the data for the proposed site by interpolation or extrapolation, taking into account differences between the proposed site and the sites for which measurements are available.

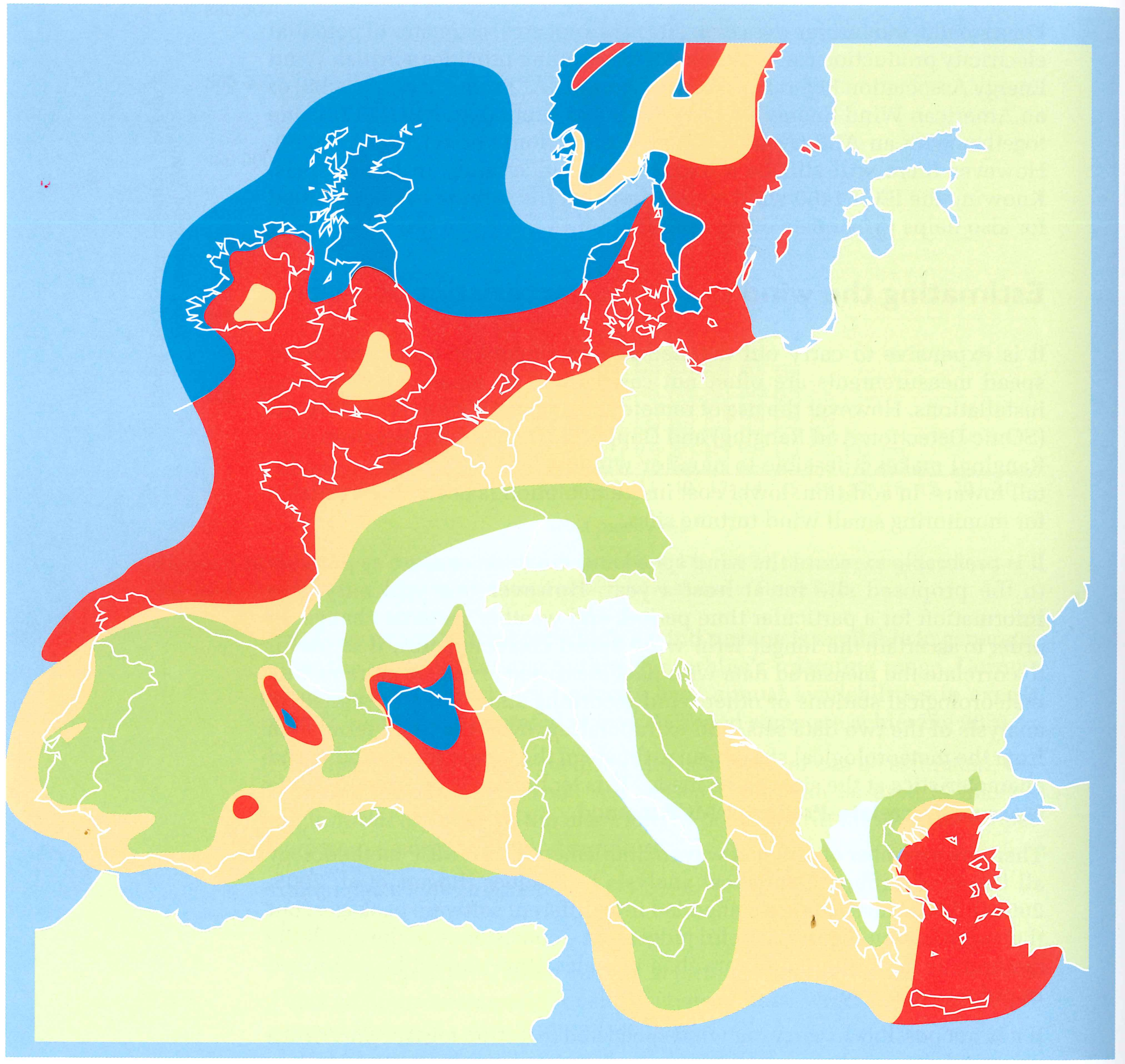

Wind resources at 50 m above ground level for five different topographic conditions											
Wind class		Sheltered terrain		Open plain		At a sea coast		Open sea		Hills and ridges	
		m s^{-1}	W m^{-2}	m s^{-1}	W m^{-2}	m s^{-1}	W m^{-2}	m s^{-1}	W m^{-2}	m s^{-1}	W m^{-2}
5		>6.0	>250	>7.5	>500	>8.5	>700	>9.0	>800	>11.5	>1800
4		5.0–6.0	150–250	6.5–7.5	300–500	7.0–8.5	400–700	8.0–9.0	600–800	10.0–11.5	1200–1800
3		4.5–5.0	100–150	5.5–6.5	200–300	6.0–7.0	250–400	7.0–8.0	400–600	8.5–10.0	700–1200
2		3.5–4.5	50–100	4.5–5.5	100–200	5.0–6.0	150–250	5.5–7.0	200–400	7.0–8.5	400–700
1		<3.5	<50	<4.5	<100	<5.0	<150	<5.5	<200	<7.0	<400

Figure 8.31 Annual mean wind speeds and wind energy resources over Europe (EU countries) combining land-based and offshore wind atlases (source: Troen and Petersen, 1989)

Using wind speed maps and atlases

Maps are available that give estimates of the mean wind speeds over the UK and many other countries. However, most of these maps were made using data from meteorological stations, which tend to be located in places that are often not appropriate for wind energy, so wind speed maps and atlases specifically for wind energy purposes have also been developed for many countries.

Using long-term wind measurements and the WAsP model mentioned below, a *European Wind Atlas* (Troen and Petersen, 1989) has been produced by the Risø Laboratory in Denmark for the European Commission. This document includes maps of various areas within the European Union (for example, Figure 8.31), which show the annual mean wind speed at 50 m above ground level for five different topographic conditions: sheltered terrain, open plain, sea coast, open sea, hills and ridges. The atlas includes a series of procedures for taking account of site characteristics to estimate the wind energy likely to be available. These procedures work quite well on sites with a gentle topography but are not so good for very hilly terrain or urban areas. A similar atlas (included in Figure 8.31) has also been produced to cover the *offshore* wind energy resource in the European Union (Risø, 2009). Similar wind atlases based on the same approach have also been produced for Russia, South Africa and parts of North Africa as well as a Global Wind Atlas. Also wind speed/energy atlases have been produced for Ireland, USA and Canada. There is a new higher resolution European Wind Atlas currently under development.

The Energy Technology Support Unit (ETSU) also prepared a wind atlas and database of the UK. Using wind speed data from meteorological stations, a digital terrain model of the UK and a wind speed prediction computer model known as NOABL (Numerical Objective Analysis of Boundary Layer), ETSU estimated an annual mean wind speed (AMWS) value for each 1 km × 1 km Ordnance Survey grid square in the UK (Burch and Ravenscroft, 1992). Whilst this is a useful atlas/database for rural areas, it consistently over predicts the AMWS in urban and suburban areas and (like most wind atlases developed for wind energy development in windy areas) it should not be used for that purpose. The UK Microgeneration Installation Standard, MIS 3003, (MIS, 2015 and MCS, 2015), include some adjustment factors that try to take account of this for small or micro wind turbines, but it is still not very reliable when used in those situations. This atlas is no longer being updated, but, at the time of writing, can still be accessed via the RenewableUK and Department for Climate Change (DECC) websites (RenewableUK, 2017; DECC, 2017).

Because of the unreliability of the NOABL database, the UK Energy Savings Trust has made available the wind speed data for Scotland that it accumulated whilst carrying out field trials of domestic small wind turbines. This database of AMWS can be accessed by entering a Scottish postcode together with the rural, suburban or urban site classification (EST, 2016).

Table 8.5 gives a summary of the wind energy capacity needed to meet the European Commission's SET-Plan targets.

Table 8.5 Wind energy capacity needed to meet the European Commission's SET-plan targets

	Onshore wind (GW)	Offshore wind (GW)	Total wind energy capacity (GW)	Average capacity factor onshore	Average capacity factor offshore	TWh onshore	TWh offshore	TWh Total	EU-27 gross electricity consumption*	Wind power's share of electricity demand
2020**	210	55	265	26.0%	42.3%	479	204	683	3494	20%
2030	250	150	400	27.0%	42.8%	592	563	1155	3368	34%
2050	250	350	600	29.0%	45.0%	635	1380	2015	4000	50%

* Electricity demand assumes the European Commission's New Energy Policy $100 oil/barrel scenario until 2020 and High Renewables/Energy Efficiency scenario for 2030. Demand in 2050 is assumed to be 4000 TWh.

** Assuming 265 GW by 2020 in accordance with EWEA's 'high' scenario combined with the European Commission's 'New Energy Policy' Assumption for demand.

Source: Zervos and Kjaer, 2009

8.9 Offshore wind energy

The capital costs of energy from offshore wind farms are generally higher than those of onshore installations because of the extra costs of civil engineering for substructure, higher electrical connection costs and the higher specification materials needed to resist the corrosive marine environment.

However, offshore wind speeds are generally higher and more consistent than on land (apart from certain mountain and hill tops) and test results from the Tunø Knob offshore wind farm in Denmark indicate that actual output is 20–30% higher than estimated from wind speed prediction models. Availability was also higher than expected with an average of 98% being achieved, though this may not necessarily be typical. These wind energy characteristics, together with likely reductions in offshore costs as experience is gained in this environment, are expected to make offshore wind energy costs competitive in the medium to long term (although it should also be noted that capital costs doubled in the five years up to 2009 (Willow and Valpy, 2011)). In deeper water, further offshore, capital and operational costs will be higher, but it is anticipated that the increased energy yield, particularly from larger rotors (offshore, it is more feasible to utilize very large-scale wind turbines than it is on land, see Box 8.5) will more than compensate for these additional costs (Willow and Valpy, 2011) though this may depend on the proportion of novel and untested engineering approaches that get deployed – especially in deeper more turbulent waters.

Europe is the world's leader in offshore wind, having installed 3230 offshore turbines (over 11027.3 MW in 84 wind farms) with grid connections to 11 European countries by the end of 2015, in shallow waters – depths mainly up to 30–45 m (EWEA, 2016). EWEA forecasts that once the six offshore projects under construction are completed a further 1.9 GW of capacity will be added, bringing the cumulative installed capacity in Europe to 12.9 GW. EWEA has identified 26.4 GW of consented offshore projects that could be constructed over the next decade. A total of 63.5 GW of projects are understood to be in the planning phase (EWEA, 2016).

BOX 8.5 Very large turbines

(a) (b) (c) (d)

Figure 8.40 (a) and (b) The 164 m diameter MHI-Vestas V164-8 MW wind turbine designed for offshore operation which employs British made blades produced on the Isle of Wight. These turbines are currently being installed in large numbers on various UK offshore wind farms. (Source: MHI-Vestas, 2016). (c) The 8 MW 154 m diameter Siemens SWT-8-154 prototype direct drive turbine being tested at the Østerild test site, Denmark, installed 30 January 2017 (source: Siemens, 2017). (d) The 7MW 167 m diameter MHI MT7167/7.0 Hydraulic drive wind turbine (or Digital Displacement Transmission (DDT) turbine) being tested at the Hunterston test site in Scotland. Currently this has the world's largest rotor diameter employing 81.6 m blades (source: MHI, 2015)

It is more feasible to utilize very large-scale wind turbines offshore than on land. This may improve economic viability, as more energy can be captured from a single platform (also known as 'power per tower') and this can have benefits in terms of reduced maintenance costs. However, working against these benefits is the tendency to increasing capital costs associated with turbines above approximately 2 MW rated capacity. The latter effect is due to the scaling laws for strength and weight of materials with increasing rotor swept area, together with the much higher torque loading experienced by gearboxes.

Very large turbines include the 150 m diameter GE (formerly Alstom) Haliade 150–6 MW, 154 m diameter Siemens 154–7 MW/8 MW (Figure 8.40(c)), 164 m diameter MHI-Vestas V164–8 MW (Figure 8.40 (a) and (b)) employing 80 m long blades developed on the Isle of Wight and manufactured on the island. During its testing phase the V164–8 MW turbine generated 192 MWh in a 24 hour period (October 2014) and as of December 2016, 32 MHI-Vestas V164–8 MW turbines were installed in 3 months on the Burbo Bank Extension project off the coast of Liverpool.

At the time of writing the turbine with the largest diameter is the 167 m diameter Mitsubishi 7 MW Hydraulic Drive Turbine (HDT) or Digital Displacement Transmission (DDT) Turbine (Figure 8.40(d)) – formerly known as the SeaAngel turbine – being tested at Hunterston in Scotland and also on a floating platform in Japan. In contrast to the latest Haliade and Siemens turbines that employ direct drive generators, the Mitsubishi 7 MW HDT utilizes a novel high efficiency hydraulic transmission system developed in the UK by Artemis Intelligent Power and based on the ideas of Professor Stephen Salter. The drive avoids the difficulties experienced by gearboxes and reduces the tower top mass which may be a critical feature in the viability of very large scale floating wind turbine systems. Subject to test results Mitsubishi (MHI) also plans to incorporate the hydraulic drive into future MHI-Vestas V164-8MW turbines.

UK based Blade Dynamics (now part of GE) developed a modular 78 m blade which was successfully tested at the ORE-Catapult test centre at Blyth, HAWT. LM Wind Power (now also part of GE) produced an 88.4 m blade in June 2016 for a 180 m diameter 8 MW wind turbine for Adwen (now part of a merged Siemens-Gamesa company).

Hendrik Stiedal (former CTO of Siemens) revealed that Siemens has produced a design for a 10 MW turbine which would have a 210 m diameter rotor, 140 m tall tower, innovative direct drive generator and predicted to generate 50 000 MWh per year (Stiedal, 2014).

AMSC Wintec Solutions has developed a design for a 190 m diameter 10 MW HAWT called SeaTitan based on an innovative super-conductor-based direct drive generator which is said to substantially reduce the tower top mass compared to other systems. At the time of writing a SeaTitan has yet to be installed.

Enercon has been manufacturing 126 m diameter 7.5 MW direct drive turbines for land-based applications.

Designs for 15 MW turbines are being considered for offshore applications by both GE and Gamesa.

The EU funded a five year long wide-ranging UpWind project to investigate and evaluate the practicality of developing 20 MW HAWTs for offshore operation. The project included 40 partners from the wind turbine industry, universities and others fields, and in the final report they concluded that such turbines (which would have rotor diameters of over 200 m) are feasible, though the blades would have to be lighter and would be more flexible than today's largest turbine blades.

Sandia Laboratories in the USA has been designing 100 m long blades for a 13 MW HAWT and are also leading a project to develop a 50 MW 'exoscale' offshore wind turbines known as 'Segmented Ultralight Morphing Rotor' (SUMR) funded by the US Department of Energy. The 200+ m long blades would morph (flex inward) in high winds.

It is uncertain how much larger horizontal axis turbines can be scaled. This will involve developing blades which will have to be lighter and have improved fatigue resistance, because when HAWTs are built to the sizes necessary to achieve very high power ratings, the reversing gravity loads on the rotor (as the blades move up and downwards during their rotation cycles) become a significant structural limitation.

Similarly, there may be an increase in the cyclic impact on large HAWT wind turbine blades due to higher levels of 'wind shear' that occur with large rotor diameters. As wind speed increases with height, the blade tip of a large diameter HAWT will move through wind velocities that vary in magnitude between the upper and lower parts of the rotation cycle and the larger the diameter the greater is the difference in wind speed experienced. Design feasibility studies are underway to explore whether larger HAWTs up to 20 MW are possible and to explore the benefits of material substitution together with improvements to the structural design of blades.

An alternative strategy is the use of multi-rotor turbines. These have been attempted periodically in the past but have not been successful commercially to date, though they may be a potential way to maximize the 'power per tower' and avoid some of the scaling issues of very large turbines mentioned above, such as high gravitational cyclic loading and high torque etc. In spite of this there are several challenges related to yawing, rotor interactions, balancing the rotor loads etc., but there are a number of projects underway to explore this approach.

Vertical axis wind turbines do not experience the gravity-driven fatigue loading encountered in large HAWTs. VAWT blades are also not as greatly affected by wind shear generated cyclic loading, and towers for some large swept area VAWT designs do not have to be built as tall in order to provide sufficient clearance above the sea level – thus reducing overturning moments. So in principle, VAWTs could be scaled-up to potentially very large sizes.

The 2009 EEA study (EEA, 2009) mentioned previously estimates that the 'economically competitive' European offshore wind energy potential 'in 2020 is 2600 TWh y^{-1}, equal to between 60% and 70% of projected electricity demand, rising to 3400 TWh y^{-1} in 2030 equal to 80% of the projected EU electricity demand.' EEA, 2009, also estimates the technical potential of offshore wind energy to be 'seven times greater than the projected EU electricity demand in 2030'.

When realized, the ambitious programmes for substantial offshore projects established by several European countries will mean that wind power will ultimately become a major provider of electricity in those countries.

One interesting development which has taken place in Norway was an innovative floating 2.3 MW wind turbine (Figure 8.42(b)), known as the Hywind project, that was successfully operated in a sea water depth of 220 m. This has significant implications for expanding the potential offshore wind energy beyond the shallow continental shelf sites so far developed. Hywind 2, a 30 MW floating pilot wind farm – at a depth of 95–120 m – is currently being developed near Peterhead using a scaled-up Hywind employing 6 MW Siemens wind turbines (Figure 8.43). See Box 8.6, which discusses floating wind turbines in more detail.

Several Asian countries, including China, Japan, Taiwan and South Korea are stimulating offshore wind energy development in their territorial waters (see Figure 8.44 and Table 8.7). China is currently the leading market for offshore wind energy in Asia with 3% of global offshore wind energy installed, it has plans to install 10 GW by 2020. Prompted by the Fukushima nuclear power plant meltdown, the Japanese government has committed to actively develop offshore wind energy, but as the coastal waters are deep the main focus has been on floating turbines. South Korea installed its first offshore wind turbines in 2012 and the government plans a phased development of a 2500 MW offshore project and 500 MW of projects are in the pipeline. Taiwan has also announced plans to deploy 600 MW of capacity by 2020 and 4 GW by 2030. India is reportedly planning some pilot offshore projects that could be operational by 2019 (Smith et al., 2015).

Whilst the USA has the world's second largest installed land-based wind energy capacity, the first US offshore wind farm – 30 MW Block Island Wind Farm off the coast of New England – began operating in December 2016. A major study of the offshore wind energy potential around the USA was completed by the National Renewable Energy Laboratory (NREL). The US offshore wind energy resource study assumed 3 MW/km^2 spacing and was based on 6 MW turbines and a 100 m hub height. Taking into account a range of constraints including water depth and exclusion zones, the US Technical offshore wind energy capacity was estimated at 2058 GW and calculated to generate some 7203 TWh/year - which is roughly double the 3863 TWh of electricity used in the USA 2014 (Musial et al., 2016).

BOX 8.6 Floating wind turbines

Floating wind turbines present a new way to access a previously unattainable clean renewable resource, namely wind energy resources at sea at water depths too deep for fixed bottom-mounted offshore wind turbines.

The potential wind energy resources at deep water locations is truly enormous so consequently there is considerable activity ongoing to develop viable floating wind energy systems. There over 30 concepts currently being developed, principally in Europe, Japan and the USA based largely on conventional horizontal axis wind turbines but a few have proposed vertical axis designs. Most of the projects are designed around a single wind turbine, though a number have proposed multi-wind turbine platforms. The concepts are generally based on a variation of three main types of floating platforms developed by the offshore oil and gas industries known as 'semi-submersible', 'spar-buoy' and 'tension leg platform' or TLP (Figure 8.41).

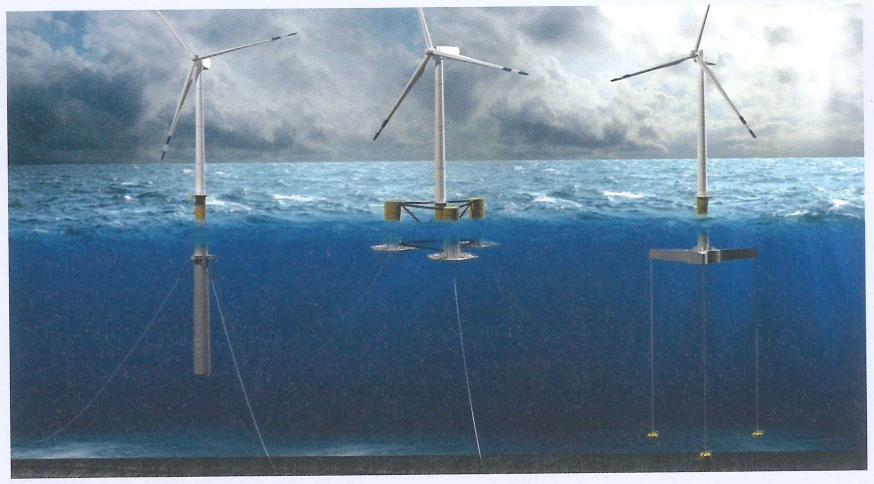

Figure 8.41 Different types of floating wind turbine platforms. Spar (left), Semi-submersible (centre) and Tension leg platform of TLP (right). (Source: DNV-GL 2016)

Prototype or demonstration floating wind turbine units based on semi-submersible and spar-type have been successfully tested in Europe, Japan and the USA (Figure 8.42). These demonstrations have helped to grow confidence in the concept and more ambitious experimental floating wind projects are in the process of being developed and deployed.

The initial prototype projects were utilising turbines rated at under 2 MW, but the current round of experimental floating wind turbine projects are utilizing much larger wind turbines such as the five Siemens 6 MW turbines on spar-buoys employed on the Statoil Hywind-Scotland project (Figure 8.43) and the 167 m diameter Mitsubishi 7 MW Hydraulic Drive Turbine – mentioned in Box 8.5 – being deployed on a V shaped semi-submersible floating platform in Japan (Figure 8.42(d)).

There are some major floating wind projects being planned around the world.

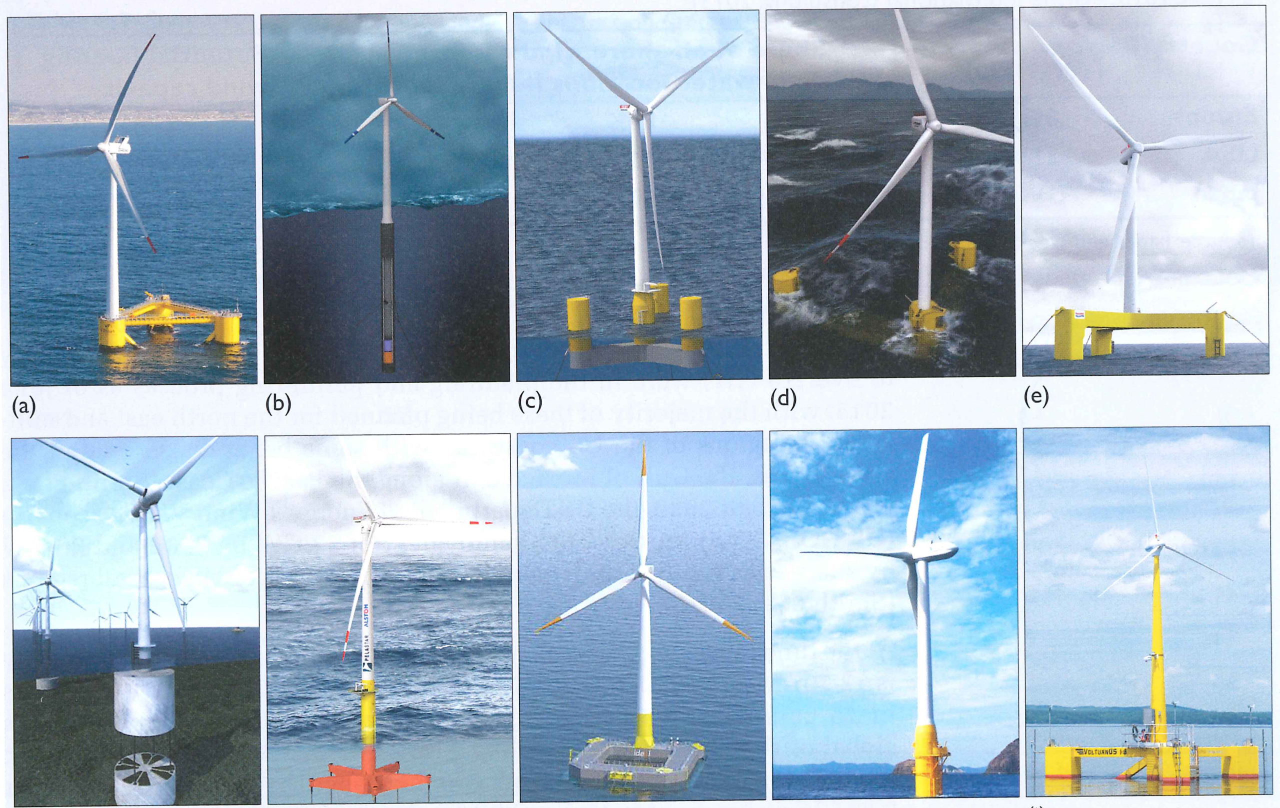

(a) (b) (c) (d) (e)
(f) (g) (h) (i) (j)

Figure 8.42 Selection of various floating wind turbine concepts being investigated and under development. (a) Principle Power WindFloat 8 MW (b) Statoil Hywind 2 MW scaling to 6 MW Siemens for Scotland (c) DCNS SeaReed 6 MW GE Haliade turbine (d) Mitsubishi Hydraulic Drive 7 MW on Fukishima Forward II Semi-sub, Japan (e) GustoMSC Tri-Floater with 5 MW wind turbine, Netherlands/France (f) DBD Systems Eco TLP (g) PelaStar TLP (Glosten) GE Haliade 6 MW turbine (h) Ideol FloatGen 2 MW, France (i) Toda Consortium-Hitachi 5 MW on hybrid spar, Japan (j) Aqua Ventus/VolturnUS University of Maine, USA

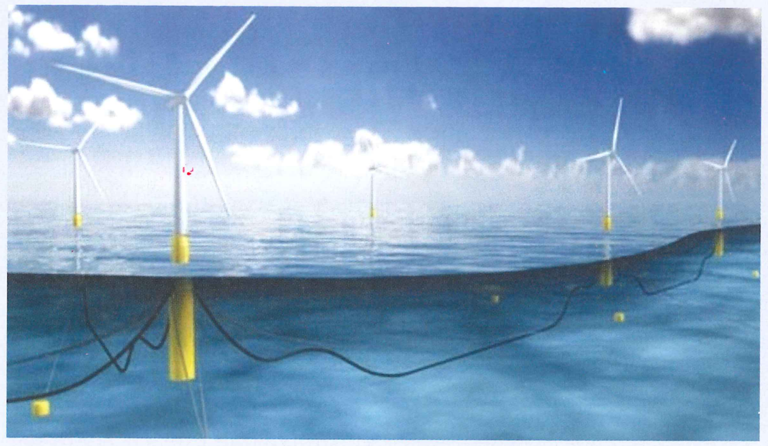

Figure 8.43 Statoil Hywind – Scotland floating wind farm planned off Peterhead. 5 × 6 MW Siemens wind turbine on spar buoy floating platforms. (Source: Statoil)

Floating VAWTs

Whilst floating VAWT concepts are being researched in various locations, the most comprehensive research is being carried out by Sandia Laboratories in the USA. They are investigating the technical and economic feasibility of floating VAWTs and have carried out detailed aerodynamic and structural rotor design studies and are progressing VAWT-specific floating platform designs, system-level studies and VAWT LCOE modelling. The main focus has been on the use of the curved blade Darrieus VAWTs, though they are also investigating other VAWT configurations and recently concluded: 'Despite technical challenges associated with floating VAWTs, the systems have inherent advantages over floating HAWTs for reducing capital costs and reducing life-cycle O&M costs.' (Griffith et al., 2016).

Floating Wind Potential

Table 8.6 Offshore wind resource potential floating wind capacity in Europe, USA, and Japan (US NREL, 2013; EWEA, 2013; Marine International Consulting, 2013).

Country/Region	Share of off-shore wind resource in deep water locations (>60m depth)	Potential floating wind capacity
Europe	**80%**	**4000 GW**
USA	**60%**	**2450 GW**
Japan	**80%**	**500 GW**

(Source: James and Costa Ros, 2015).

About 210 US offshore wind energy projects (with a combined capacity of over 15 GW) were in the planning and permitting process as of June 2015, with the majority of these being planned for the north east and mid-Atlantic regions of the US coastline, with some being considered at the Great Lakes, the Gulf of Mexico and along the Pacific Coast (Smith et al., 2015). Beyond 2020, the US Department of Energy's Wind Vision scenario (US DOE, 2015) includes the deployment of 22 GW by 2030 and 86 GW by 2050, with future deployment occurring in all major US coastal regions (Smith et al., 2015).

At the time of writing the total current global offshore wind energy capacity is 12 107 MW, installed with 2739 turbines across 73 offshore wind farms in 15 countries, with 92% in European waters. Current policy plans global offshore wind capacity to reach 72 GW in 2030 (WEC, 2016), with another 460 MW installed (not yet commissioned) by end of 2015, a further 2.56 GW under construction and 8.13 in pre-construction stages. According to the Global Offshore Wind Farm Database (4C Offshore, 2016), over 900 offshore wind farms are being planned in 36 countries around the world. Table 8.7 and Figure 8.44 summarize the global offshore wind projects as of June 2015. Ernst & Young have projected that by 2020, offshore wind will be about 10% of global installed capacity (Ernst & Young, 2015).

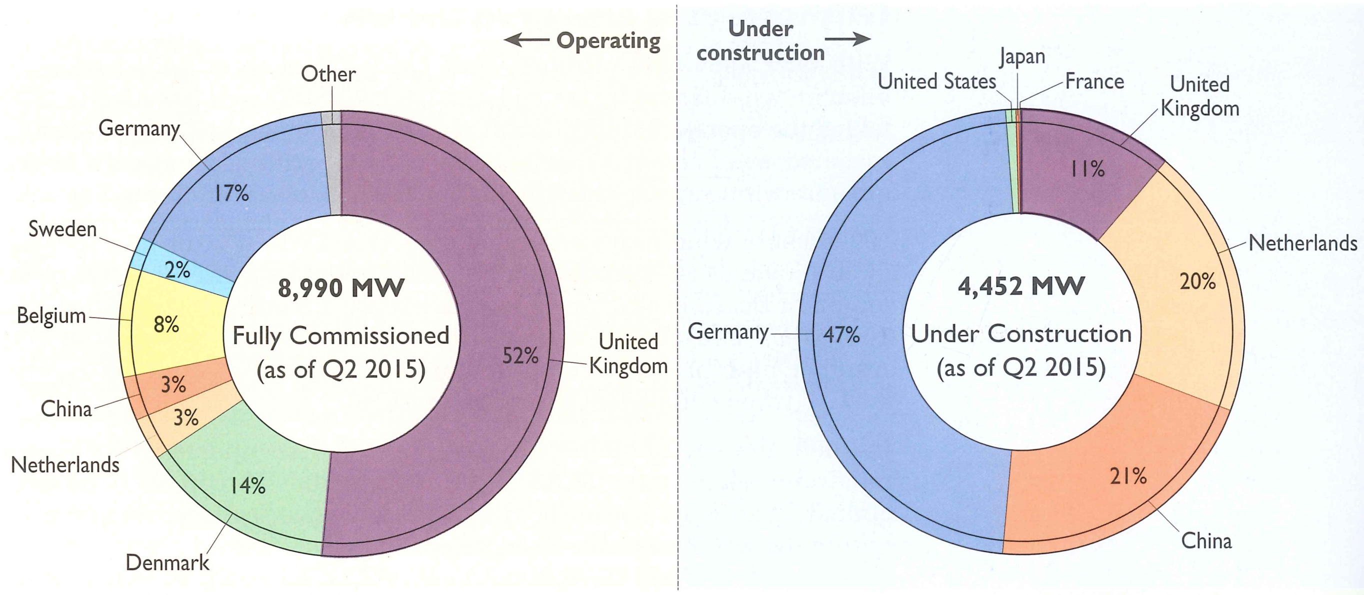

Figure 8.44 Global offshore wind power capacity by country as of June 2015. Left: Fully commissioned. Right: Under construction (source: Smith et al., 2015)

Table 8.7 Summary of Operating and Under Construction Offshore Wind Projects by Country (as of 30 June 2015)

	Operating (MW)	Under Construction (MW)	Total (MW)	Rank
United Kingdom	4625	503	5128	1
Germany	1505	2108	3613	2
Denmark	1271	0	1271	3
China	310	918	1228	4
Netherlands	247	873	1120	5
Belgium	712	0	712	6
Sweden	202	0	202	7
Japan	52	13	64	8
Finland	32	0	30	9
United States	0	30	30	10
Ireland	25	0	25	11
France	0	8	8	12
South Korea	5	0	5	13
Norway	2	0	2	14
Portugal	2	0	2	15
Total	8990	4452	13442	

Note: Totals may not sum due to rounding.

References

4C Offshore (2010) *4C Offshore* [Online]. Available at http://www.4coffshore.com (Accessed 8 January 2010).

4C Offshore (2016) *Offshore Wind Overview Report*, [Online], Lowestoft, Suffolk, 4C Offshore Ltd. Available at http://www.4coffshore.com/windfarms/downloads/samples/20160404_OverviewReportSample.pdf (Accessed 24 February 2017).

Abbott, I. H. and von Doenhoff, A. E. (1958) *Theory of Wing Sections*, New York, Dover Publications Inc.

ABC (2011) *American Bird Conservancy (ABC) policy on bird collisions*, [Online]. Available at http://www.abcbirds.org/abcprograms/psolicy/collisions/index.html (Accessed 8 November 2011).

AOA (2016) *Safeguarding of Aerodromes: Advice Note 5 Renewable Energy and Impact on Aviation*, [Online], London, Airport Operators Association. Available at http://www.aoa.org.uk/wp-content/uploads/2016/09/Advice-Note-5-Renewable-Energy-2016.pdf (Accessed 24 February 2017).

Appleton, S. (2010) *Stealth blades – a progress report*, [Online], Glasgow, All-Energy Available at http://onlinelibrary.wiley.com/doi/10.1029/2004JD005462/full (Accessed 20 March 2017).

Archer, C. L. and Jacobson, M. Z. (2005) 'Evaluation of global wind power', *J. Geophys Res.*, 110, D12110, [Online]. Available at http://www.agu.org/journals/jd/ jd0512/2004JD005462/ (Accessed 8 November 2011).

ASI (2013) *Aviation Planning Considerations for Wind Turbines: Managing the Impact of Wind Turbines on Aviation*, [Online], London, Airspace & safety initiative. Available at http://airspacesafety.com/wp-content/uploads/2013/09/20130701ManagingTheImpactOfWindTurbinesOnAviation_Script_FINAL_V1.pdf (Accessed 24 February 2017).

AWEA (2009) *AWEA Small Wind Turbine Performance and Safety Standard* – AWEA 9.1 [Online], Washington, American Wind Energy Association. Available at smallwindcertification.org/wp-content/uploads/2011/05/AWEA_2009-Small_Turbine_Standard1.pdf (Accessed 9 January 2017).

AWWI (2016) *Wind Turbine Interactions with Wildlife and their Habitats: A Summary of Research Results and Priority Questions*, [Online], Washington, American Wind & Wildlife Institute. Available at https://awwi.org/wp-content/uploads/2016/07/AWWI-Wind-Wildlife-Interactions-Summary-June-2016.pdf (Accessed 21 December 2016).

Bacon, D. F. (2002) *Fixed-link wind turbine exclusion zone method, A proposed method for establishing an exclusion zone around a terrestrial fixed radio link outside of which a wind turbine will cause negligible degradation of the radio link performance*, [Online], London, Ofcom. Available at https://www.ofcom.org.uk/__data/assets/pdf_file/0031/68827/windfarmdavidbacon.pdf (Accessed 1 February 2017).

Barrett, S. B. and DeVita, P. M (2011) *Investigating Safety Impacts of Energy Technologies on Airports and Aviation – A Synthesis of Airport Practice*, ACRP Synthesis 28, [Online], Washington, Transport Research Board. Available at www.TRB.org (Accessed 24 February 2017).

Barrett, S. B., DeVita, P. M. and Lambert, J. R. (2014) *Guidebook for Energy Facilities Compatibility with Airports and Airspace*, ACRP Report 108, [Online], Washington, Transportation Research Board. Available at www.TRB.org (Accessed 24 February 2017).

BBC (2016) *Windfarm Assessment Tool* [Online]. Available at http://www.bbc.co.uk/reception/info/windfarm_tool.html (Accessed 12 December 2016).

BCT (2009) *Determining the potential ecological impact of wind turbines on bat populations in Britain, Phase 1 report Final Report*, [Online], Scoping & Method Development Report, May. Available at www.bats.org.uk/pages/wind_turbines.html and http://www.bats.org.uk/data/files/determining_the_impact_of_wind_turbines_on_british___bats_final_report_29.5.09_website.pdf (Accessed16 March 2017).

BCT (2010) *Position Statement: Microgeneration Schemes: Risks, Evidence and Recommendations* [Online], London, Bat Conservation Trust. Available at http://www.bats.org.uk/publicatio ns.php?keyword=microgeneration+schemes&month=&year=&category=&search=Search (Accessed 9 July 2017).

BCT (2017) *Microgeneration Schemes*: A Position Statement from BCT, [Online], Bat Conservation Trust. http://www.bats.org.uk/pages/microgeneration_issues.html (Accessed 16 March 2017).

BEIS (2013) *Wind turbines, aviation and radar, Onshore wind: part of the UK's energy mix* [Online]. Available at https://www.gov.uk/guidance/onshore-wind-part-of-the-uks-energy-mix (Accessed on 19 December 2016).

BEIS (2016) *Energy and Climate Change Public Attitude Tracker – Wave 19*, [Online]. London, UK Department for Business, Energy & Industrial Strategy (BEIS), Available at https://www.gov.uk/government/uploads/system/uploads/attachment_data/file/563236/Summary_of_key_findings_BEIS_Public_Attitudes_Tracker_-_wave_19.pdf, and accompanying *Wave 19 Summary Tables* spreadsheet, https://www.gov.uk/government/statistics/public-attitudes-tracking-survey-wave-19, (Accessed 3 January 2017).

Berge, E., Gravdahl, A. R., Schelling, J., Tallhaug, L. and Undeheim, O (2006) *A comparison of WAsP and two CFD-models*, [Online]. Presentation for EWEC 2006 Available at http://www.windchina.info/cwpp/files/1613/9821/8733/WAsPCFD_WAsP_WindSim_ewec_berge.pdf (Accessed February 2017).

BERR (2008) *Atlas of UK Marine Renewable Energy Resources*, [Online]. Southampton, Department for Business & Regulatory Reform, Available at http://www.renewables-atlas.info (Accessed 17 March 2017).

Beurskens, J. and Jensen, P. H. (2001) 'Economics of wind energy – Prospects and directions', *Renewable Energy World*, July–Aug.

Bright, J. A., Langston, R. H. W., Bullman, R., Evans, R. J., Gardner, S., Pearce-Higgins, J. and Wilson, E. (2006) *Bird Sensitivity Map to provide locational guidance for onshore wind farms in Scotland, RSPB Research Report No 20* [Online], Sandy, Bedfordshire, Royal Society for the Protection of Birds.

Available at https://www.rspb.org.uk/Images/sensitivitymapreport_tcm9-157990.pdf (Accessed 24 February 2017).

Bright, J. A., Langston, R. H. W. and Anthony, S. (2009) *Mapped and written guidance in relation to birds and onshore wind energy development in England, RSPB Research Report No 35* [Online], Sandy, Bedfordshire, Royal Society for the Protection of Birds. Available at http://www.rspb.org.uk/Images/EnglishSensitivityMap_tcm9-237359.pdf (Accessed 24 February 2017).

BSI (2013) Wind turbines: Acoustic noise measurement techniques, (BS) EN 64100-11:2013, London, British Standards Institution.

Burch, S. F. and Ravenscroft, F. (1992) *Computer Modelling of the UK Wind Energy Resource: Final Overview Report*, ETSU WN7055, ETSU Oxon, Crown copyright.

Burroughs, W. J., Crowder, B., Robertson, E., Vallier-Talbot, E. and Whitaker, R. (1996) *Weather – the ultimate guide to the elements*, London, HarperCollins.

Butler, G. (2007) 'Advanced Digital Tracker – Update' at All Energy '07 Aviation and technical Workshop, May http://www.all-energy.co.uk/UserFiles/File/2007GeoffButler.pdf (Accessed 9 December 2011).

BWEA (2008) BWEA Small Wind Turbine Performance and Safety Standard, 29 February. Available at https://www.solarcollect.co.uk/downloads/bwestandard2008.pdf (Accessed 17 March 2017).

CAA (2010) *Lighting of En-Route Obstacles and Onshore Wind Turbines*, Policy Statement, [Online], London, Directorate of Airspace Policy, Civil Aviation Authority. Available at https://publicapps.caa.co.uk/docs/33/DAP_LightingEnRouteObstaclesAndWindTurbines.pdf (Accessed 24 February 2017).

CAA (2015) *ACN-2015-00-0460: Liverpool Windfarm Trial (AL1)*, [Online], London, Safety & Airspace Regulations Group, Civil Aviation Authority. Available at https://publicapps.caa.co.uk/docs/33/2015000460ACN11LverpoolWindfarmTrial.pdf (Accessed 24 February 2017).

CAA (2016) *CAP 764 - CAA Policy and Guidelines on Wind Turbines*, Safety & Airspace Regulations Group, [Online], London, Civil Aviation Authority. Available at https://publicapps.caa.co.uk/docs/33/CAP764%20Issue6%20FINAL%20Feb.pdf (Accessed 24 February 2017).

Carbon Trust (2008) *Offshore wind power: big challenge, big opportunity*, [Online], London, Carbon Trust. Available at https://www.carbontrust.com/resources/reports/technology/offshore-wind-power/ (Accessed 24 February 2017).

Carbon Trust (2016) *European offshore wind developers join forces with the Carbon Trust to slash costs of offshore wind*, Press Release 11 July 2016, https://www.carbontrust.com/about-us/press/2016/07/european-offshore-wind-developers-join-forces-with-the-carbon-trust-to-slash-costs-of-offshore-wind (Accessed 17 March 2017).

Chignell, R. J. (1987) *Electromagnetic Interference from Wind turbines – A Simplified Guide to Avoiding Problems*, East Kilbride, National Wind Turbine Centre, National Engineering Laboratory.

Clark, G (2015) *House of Commons: Written Statement (HCWS42) - Local Planning*, [Online], London, Department for Communities and Local Government. Available at http://www.parliament.uk/documents/commons-vote-office/June%202015/18%20June/1-DCLG-Planning.pdf (Accessed 3 January 2017).

Cobbett, W (1830) *Rural rides in the southern, western and eastern counties of England*, London, Penguin Classics.

Corbetta, G., Ho, A. and Pineda, I. (2015) *Wind energy scenarios for 2030*, [Online], Brussels, Belgium, WindEurope. Available at https://www.ewea.org/fileadmin/files/library/publications/reports/EWEA-Wind-energy-scenarios-2030.pdf (Accessed 24 February 2017).

Crown Estate (2008a) *Round 3 offshore wind farms table*, The Crown Estate, June.

Crown Estate (2008b) *Round 3 Offshore wind farms map*, The Crown Estate, http://www.thecrownestate.co.uk/media/158181/round3_map.pdf (Accessed 8 November 2011).

Crown Estate (2012) *Offshore Wind Cost Reduction Pathways Study*, [Online], London, The Crown Estate. Available at https://www.thecrownestate.co.uk/media/5493/ei-offshore-wind-cost-reduction-pathways-study.pdf (Accessed 9 Jan 2017).

Crown Estate (2016) *Offshore wind operational report: January – December 2015*, [Online], London, Crown Estate. Available at https://www.thecrownestate.co.uk/media/5462/ei-offshore-wind-operational-report-2016.pdf (Accessed 24 February 2017).

Day, A., Dance, S., Moseley, T. and Dunlop, B. (2010) *Ashenden Wind turbine trial: Phase II Progress Report*, [Online], London, South Bank University. Available at https://www.wind-power-program.com/Library/Performance%20of%20individual%20wind%20turbine%20installations/ashenden_turbine_trial_end_of_phase_II(QR5).pdf (Accessed 24 February 2017).

DCLG (2007) *Domestic Installation of Microgeneration Equipment – Final report from a Review of the related Permitted Development Regulations*, [Online], London, Department for Communities and Local Government. Available at https://planningjungle.com/wp-content/uploads/Domestic-Installation-of-Microgeneration-Equipment-Final-report-from-a-Review-of-the-related-Permitted-Development-Regulations-April-2007-Part-1.pdf (Accessed 24 February 2017).

DCLG (2009) *Permitted development rights for small scale renewable and low carbon energy technologies, and electric vehicle charging infrastructure – Consultation*, [Online], London, Department for Communities and Local Government. Available at https://planningjungle.com/wp-content/uploads/Permitted-development-rights-for-small-scale-renewable-and-low-carbon-energy-technologies-and-electric-vehicle-charging-infrastructure-Consultati-on-November-2009.pdf (Accessed 17 March 2017).

DCLG (2011) *The National Planning Policy Framework*, [Online], London, Department for Communities and Local Government. Available at https://www.publications.parliament.uk/pa/cm201012/cmselect/cmcomloc/1526/1526.pdf (Accessed 24 February 2017).

DCLG (2012) *National Planning Policy Framework*, [Online], London DCLG. Available at https://www.gov.uk/government/uploads/system/uploads/attachment_data/file/6077/2116950.pdf (Accessed 17 March 2017).

DCLG (2013) *Planning practice guidance for renewable and low carbon energy*, [Online], London, Department for Communities and Local Government. Available at https://www.gov.uk/government/uploads/system/uploads/attachment_data/file/225689/Planning_Practice_Guidance_for_Renewable_and_Low_Carbon_Energy.pdf (Accessed 24 February 2016).

DCLG (2015) *The Town and Country Planning Order 2015, No. 596, Part 14* [Online], Surrey, The National Archives. Available at http://www.legislation.gov.uk/uksi/2015/596/pdfs/uksi_20150596_en.pdf (Accessed 24 February 2017).

DECC (2009) *the UK Renewable Energy Strategy*, [Online], London, Department of Energy and Climate Change, HMSO. Available at https://www.gov.uk/government/uploads/system/uploads/attachment_data/file/228866/7686.pdf (Accessed 24 February 2017).

DECC (2010) *2050 Pathways Analysis*, [Online], London, Department of Energy and Climate Change. Available at https://www.gov.uk/government/uploads/system/uploads/attachment_data/file/42562/216-2050-pathways-analysis-report.pdf (Accessed 24 February 2017).

DECC (2011a) *2050 Pathways Analysis – Response to Call for Evidence*, [Online], London, Department of Energy and Climate Change. Available at https://www.gov.uk/government/uploads/system/uploads/attachment_data/ile/68821/2050-pathways-analysis-response-pt1.pdf (Accessed 24 February 2017).

DECC (2011b) *The Carbon Plan: Delivering our low carbon future*, London, Department of Energy and Climate Change. Available at https://www.gov.uk/government/uploads/system/uploads/attachment_data/file/47613/3702-the-carbon-plan-delivering-our-low-carbon-future.pdf (Accessed 24 February 2017).

DECC (2015) *The Aviation Plan – In respect of the interaction of wind turbines and aviation interests*, [Online], London, Department of Energy and Climate Change. Available at https://www.gov.uk/government/uploads/system/uploads/attachment_data/file/397208/Aviation_Plan_Update_2015_FINAL.pdf (Accessed 24 February 2017).

DECC (2016) *Energy and Climate Change Public Attitude Tracker – Wave 17*, London, Department of Energy & Climate Change. Available at https://www.gov.uk/government/statistics/public-attitudes-tracking-survey-wave-17 (Accessed 24 February 2017).

DECC (2017) Department of Energy and Climate Change's wind speed database website URL: http://webarchive.nationalarchives.gov.uk/20121217150421/http:/decc.gov.uk/en/content/cms/meeting_energy/wind/onshore/deploy_data/windsp_databas/windsp_databas.aspx (Accessed 17 March 2017) or http://www.bwea.org/noabl/index.html (Accessed 17 March 2017).

DIO (2014) *Guidance – Wind farms: MOD safeguarding*, [Online], Sutton Coldfield, West Midlands, Defence Infrastructure Organisation, Ministry of Defence. Available at https://www.gov.uk/government/publications/wind-farms-ministry-of-defence-safeguarding/wind-farms-mod-safeguarding (Accessed 24 February 2017).

DNV-GL (2014) *Electrifying the Future*, Oslo, DNV-GL

Drewitt, A. L. and Langston, R. H. W. (2006) 'Assessing the impacts of wind farms on birds', *British Ornithologists' Union*, vol. 148, pp. 29–42.

EC (2009) *Investing in the Development of low Carbon technologies (SEt-Plan)*, [Online], Brussels, European Commission. Available at http://www.biofuelstp.eu/downloads/2009_comm_investing_development_low_carbon_technologies.pdf (Accessed 24 February 2017).

EEA (2009) *Europe's on shore and offshore wind energy potential – An assessment of environmental and economic constraints, EEA Technical Report No. 6/2009,* [Online], Copenhagen, European Environment Agency. Available at http://www.eea.europa.eu/publications/europes-onshore-and-offshore-wind-energy-potential (Accessed 24 February 2017).

Eldridge, F. R. (1975) *Wind Machines*, (Report to the NSF, Mitre Corporation, USA, 1975).

English Nature, RSPB, WWF-UK, BWEA (2001) *Wind farm development and nature conservation*, Sandy, Bedfordshire, RSPB.

Erickson, W., Rabie, P., Taylor, K. and Bay, K. (2015) *Comparison of avian mortality sources and evaluation and development of compensatory mitigation options for birds, National Wind Coordinating Collaborative 2014 Washington*, American Wind Wildlife Institute.

Ernst & Young (2015) *Offshore wind in Europe: Walking the tightrope to success*, [Online], France, Ernst & Young. Available at http://www.ewea.org/fileadmin/files/library/publications/reports/EY-Offshore-Wind-in-Europe.pdf (Accessed 24 February 2017).

EST (2009) *Location, location, location: Domestic small-scale wind field trial*, [Online], London, Energy Savings Trust. Available at http://www.solacity.com/docs/BEST%20turbine%20trial%20report.pdf (Accessed 24 February 2017).

EST (2016) *Wind Speed Predictor*, [Online]. http://www.windspeed.energysavingtrust.org.uk/ (Accessed 8 December 2016).

EU (2010) *The European Strategic Energy technology Plan – SET-Plan* [Online]. Available at https://ec.europa.eu/energy/en/topics/technology-and-innovation/strategic-energy-technology-plan (Accessed 24 February 2017).

Everett, B., Boyle, G. A., Peake S. and Ramage, J. (2012) *Energy Systems and Sustainability: Power for a Sustainable Future* 2nd edn, Oxford, Oxford University Press/Milton Keynes, The Open University.

EWEA (1991) *Time for Action: Wind Energy in Europe,* Brussels, European Wind Energy Association.

EWEA (2010) *2050: Facilitating 50% Wind Energy – Recommendations on transmission infrastructure, system operation and electricity market integration*, [Online], Brussels, European Wind Energy Association. Available at http://www.ewea.org/fileadmin/files/library/publications/position-papers/EWEA_2050_50_wind_energy.pdf (Accessed 27 February 2017).

EWEA (2012) *Workshop on Wind Turbine Noise: From Source to Receiver,* [Online]. Available at http://www.ewea.org/events/workshops/past-workshops/wind-turbine-noise/ (Accessed 12 December 2016).

EWEA (2014) *Saving water with wind energy* [Online], Brussels, European Wind Energy Association. Available at https://windeurope.org/fileadmin/files/library/publications/reports/Saving_water_with_wind_energy.pdf (Accessed 27 February 2017).

EWEA (2016) *The European offshore wind industry – key trends and statistics 2015* [Online], Brussels, European Wind Energy Association. Available at https://www.ewea.org/fileadmin/files/library/publications/statistics/EWEA-European-Offshore-Statistics-2015.pdf (Accessed 27 February 2017).

Fields, J., Oteri, F., Preus, R. and Baring-Gould, I. (2016) *Deployment of Wind Turbines in the Built Environment: Risks, Lessons, and Recommended Practices* [Online], Washington, National Renewable Energy Laboratory. Available at http://www.nrel.gov/docs/fy16osti/65622.pdf

Fiumicelli, D. and Triner, N. (2011) *Wind Farm Noise Statutory Nuisance Complaint Methodology* [Online], Beckenham, AECOM for DEFRA. Available at https://www.gov.uk/government/uploads/system/uploads/attachment_data/file/69222/pb-13584-windfarm-noise-statutory-nuisance.pdf (Accessed 27 February 2017).

FWC (2017) *Floating windfarms corporation* [Online]. Available at http://floatingwindfarms.com/index.html (Accessed 31 January 2017).

Golding, E. W. (1955) 'Generation of Electricity by Wind Power', London, E. and F. N. Spon.

Gorlov, A. (1998) *Development of the helical reaction hydraulic turbine, Final Technical Report (DE-FG01-96EE 15669)*, [Online], Washington, Northeastern University for US Department of Energy. Available at https://www.osti.gov/scitech/servlets/purl/666280/ (Accessed 27 February 2017).

Greenacre, P., Gross, R. and Heptonstall, P. (2010) *Great Expectations: the cost of offshore wind in UK waters – understanding the past and projecting the future*, London, UK Energy Research Centre.

Greenblatt, J. B. (2005) *Wind as a source of energy, now and in the future*, Amsterdam, Environment Defense for InterAcademy Council.

Griffiths, T., Paquette, J., Barone, M., Owens, B. and Bull, D. (2016) 'Floating Offshore Vertical Axis Wind Turbine Project', Poster presented at *AWEA 2016*, SAD2016-4691C, Sandia National Laboratories.

Grubb, M. and Meyer, N. (1993) *Wind energy: resources, systems and regional strategies*, in Johansson, T.B. et.al (eds) Renewable Energy – Sources for Fuels and Electricity, Washington, Island Press.

GWEC (2016a) *Global Wind Report – Annual Market Update for 2015*, [Online]. Available at http://www.gwec.net/wp-content/uploads/vip/GWEC-Global-Wind-2015-Report_April-2016_19_04.pdf (Accessed 19 March 2017).

GWEC (2016b) *Global Wind Energy Outlook – 2016*, [Online]. Available at http://www.gwec.net/publications/global-wind-energy-outlook/global-wind-energy-outlook-2016/ (Accessed 19 March 2017). (Accessed 27 February 2017).

Hayhow, D. B., Burns, F., Eaton, M. A., Al Fulaij, N., August, T. A., Babey, L., Bacon, L., Bingham, C., Boswell, J., Boughey, K. L., Brereton, T., Brookman, E., Brooks, D. R., Bullock, D. J., Burke, O., Collis, M., Corbet, L., Cornish, N., De Massimi, S., Densham, J., Dunn, E., Elliott, S., Gent, T., Godber, J., Hamilton, S., Havery, S., Hawkins, S., Henney, J., Holmes, K., Hutchinson, N., Isaac, N. J. B., Johns, D., Macadam, C. R., Matthews, F., Nicolet, P., Noble, D. G., Outhwaite, C. L., Powney, G. D., Richardson, P., Roy, D. B., Sims, D., Smart, S., Stevenson, K., Stroud, R. A., Walker, K. J., Webb, J. R., Webb, T. J., Wynde, R. and Gregory, R. D. (2016) *State of Nature 2016*, [Online], Newark, State of Nature partnership, http://www.wildlifetrusts.org/sites/default/files/state_of_nature_uk_report_pages_1_sept.pdf (Accessed 28 February 2017).

Health Canada (2014) *Wind Turbine Noise and Health Study* [Online]. Available at http://www.hc-sc.gc.ca/ewh-semt/noise-bruit/turbine-eoliennes/summary-resume-eng.php (Accessed on 28 February 2017).

IEA (2016) *World Energy Outlook* [Online]. Available at https://www.iea.org/newsroom/news/2016/november/world-energy-outlook-2016.html (Accessed 28 February 2017).

IEC (2012) *Wind turbine generator systems – Part 11: Acoustic noise measurement techniques, IEC Standard 61400-11,* Geneva, International Electrotechnical Commission.

IOA, 2013 *A good practice guide to the application of ETSU-R-97 for the assessment and rating of wind turbine noise*, [Online], St. Albans, Hertfordshire, The Institute of Acoustics. Available at http://www.ioa.org.uk/sites/default/files/IOA%20Good%20Practice%20Guide%20on%20Wind%20Turbine%20Noise%20-%20May%202013.pdf (Accessed 28 February 2017).

IOA (2016) *A Method for Rating Amplitude Modulation in Wind Turbine Noise*, [Online], St. Albans, Hertfordshire, The Institute of Acoustics. Available at http://ioa.org.uk/sites/default/files/AMWG%20Final%20Report-09-08-2016_0.pdf (Accessed 28 February 2017).

IPCC (2011) *Special Report of Renewable Energy Sources and Climate Mitigation (SEREN) - Summary Report*, Abu Dhabi, Inter-government Panel on Climate Change.

Jacobson, M. Z., Delucchi, M. A., Bauer, Z. A. F., Goodman, S. C., Chapman, W. E., Cameron, M. A., Bozonnat, C., Chobadi, L., Clonts, H. A., Enevoldsen, C. P., Erwin, J. R., Fobi, S. N., Goldstrom, O. K., Hennessy, E. M., Liu, J., Lo, J. Meyer, C. B., Morris, S. B., Moy, K. R., O'Neill, P. L., Petkov, I., Redfern, S., Schucker, R., Sontag, M. A., Wang, J., Weiner, E. and Yachanin, A. S. (2016) *100% Clean and Renewable Wind, Water, and Sunlight (WWS) All Sector Energy Roadmaps for 139 Countries of the World*, [Online], California, Stanford University. Available at https://web.stanford.edu/group/efmh/jacobson/Articles/I/CountriesWWS.pdf (Accessed 1 March 2017).

Jago, P. and Taylor, N. (2002) *Wind turbines and aviation interests – European Experience and Practice*, STAYSIS Ltd for the DTI, ETSU W/14/00624/REP (DTI PUB URN No 03/5151). [Online], Brussels, Association pour la Promotion des Energies Renouvelables. Available at http://www.apere.org/manager/docnum/doc/doc1288_aviation.fiche115 (Accessed 1 March 2017).

James, R & Costa Ros, M (2015) *Floating Offshore Wind: Market & Technology Review* [Online], London, Carbon Trust. Available at https://www.carbontrust.com/media/670664/floating-offshore-wind-market-technology-review.pdf (Accessed 1 March 2017).

Jamieson, A. (2012) *Offshore Wind Cost Reduction Task Force Report, June 2012*, [Online], London, RenewableUK. Available at https://www.gov.uk/government/uploads/system/uploads/attachment_data/file/66776/5584-offshore-wind-cost-reduction-task-force-report.pdf (Accessed 1 March 2017).

JRC (2014a) *Calculation of Wind Turbine clearance zones for JRC managed fixed services with particular reference to UHF (460MHz) Telemetry Systems when turbine sizes and locations are accurately known*, Issue 4.2, Joint Radio Company, December 2014. Available at http://www.jrc.co.uk/sites/default/files/Calculation%20of%20the%20Clearance%20Zone%204.2.1_0.pdf (Accessed 20 March 2017).

JRC (2014b) *Procedure for coordination with wind energy developments*, Issue 2.1, Joint Radio Company, December 2014. Available at http://www.jrc.co.uk/sites/default/files/JRC_Procedure_for_co-ordination_with_wind_energy_developments-2.1.0.pdf (Accessed 20 March 2017).

JRC (2016) *Radio Link Coordination with Wind Farms*, [Online]. Available at http://www.jrc.co.uk/wind-farms (Accessed 12 December 2016).

Kendrick, M. (2017) 'Does diet play a role in cardiovascular disease' presented at 2017 Public Health Collaboration Conference, Manchester, 17-18 June.

Kragh, J. et al. (1999) *Noise immission from wind turbines*, National Engineering Laboratory for the Energy Technology Support Unit (ETSU), ETSU W/13/00503/REP.

LCTU (2013) *Energy Policy Toolkit on Physical Planning of Wind Power: Experiences from Denmark*, [Online], Copenhagen, Danish Energy Agency.

Available at https://ens.dk/sites/ens.dk/files/Globalcooperation/physical_planning_of_wind_power.pdf (Accessed 1 March 2017).

Legerton, M. (ed.) (1992) *Wind turbine Noise Workshop Proceedings*, ETSU-N-123, Kirkstile, Department of Trade and Industry/British Wind Energy Association.

Ljunggren, S. and Gustafsson, A. (1994) *Recommended practices for Wind turbine testing. 4. Acoustics Measurement of Noise Emission from Wind turbines* (3rd edn), submitted to the Executive Committee of the International Energy Agency Programme for Research and Development on Wind Energy Conversion Systems.

Ljunggren, S. (1997) Recommended practices for Wind turbine testing. 10. Measurement of Noise Emission from Wind turbines, submitted to the Executive Committee of the International Energy Agency Programme for Research and Development on Wind Energy Conversion Systems.

London Array (2012) The world's largest offshore wind farm, [Online], London, London Array. Available at https://web.archive.org/web/20110920071946/http://www.londonarray.com/downloads/london_array_brochure.pdf. (Accessed 1 March 2017).

London Array (2016) *Renewable Energy Record Achieved at London Array*, [Online], London, London Array. Available at http://www.londonarray.com/project/renewable-energy-record-achieved-at-london-array/ (Accessed 1 March 2017).

Marsh, G (2010) 'Going stealthy with composites', Reinforced Plastics Magazine, November/December 2010 issue. Available at url http://www.materialstoday.com/composite-applications/features/going-stealthy-with-composites/ (accessed 1 February 2017).

Marshall, C (2016) 'Nature loss linked to farming intensity', BBC News, 14 September [Online]. Available at www.bbc.co.uk/news/science-environment-37298485 (Accessed 1 March 2017).

Mathews, F., Richardson, S., Lintott, P. and Hosken, D. (2016) *Understanding the Risk to European Protected Species (bats) at Onshore Wind Turbines to inform Risk Management*, Exeter, University of Exeter.

Mathiesen, J, (2014) 'Carbon Trust Offshore Wind Accelerator: Driving down the cost of offshore wind,' Presentation at *EERA DeepWind 2014*, http://www.sintef.no/globalassets/project/deepwind2014/presentations/closing/j-matthiesen_carbon-trust.pdf (Accessed 9 January 2017).

McMillan, D. and Ault, G. (2007) 'Quantification of Condition Monitoring Benefit for Offshore Wind Turbines', *Wind Engineering*, vol. 31, no. 4, pp. 267–285.

MCS (2009) *MCS 006 Issue 1.5 – Product certification scheme requirements: Micro and Small Wind turbines*, MCS Working Group 3 'Micro and Wind Systems' for DECC, http://www.microgenerationcertification.org/images/MCS%20006%20-%20Issue%202.1%20Product%20Certification%20Scheme%20Requirements%2015%20Jan%202014.pdf (Accessed 9 December 2011).

MCS (2015) *MCS 020 Planning standards for permitted development installations of wind turbines and air source heat pumps on domestic premises, Issue 1.2*, [Online], London, Department of Energy and Climate Change. Available at http://regulations.completepicture.co.uk/pdf/Mcs/MCS%20020%20Planning%20Standards%20Issue%201.2.pdf (Accessed 8 July 2017).

MCS (2017) *Microgeneration Certification Scheme*, [Online]. Available at www.microgenerationcertification.org (Accessed 1 March 2017).

Milborrow, D., (2013) 'Turbine advances cut O&M costs', *WindPower Monthly* magazine, 1 June [Online]. Available at www.windpowermonthly.com/article/1183992/turbine-advances-cut-o-m-costs (Accessed 9 January 2017).

MIS (2015) *MIS 3003: Issue 3.4 Microgeneration Installation Standard: Requirements for MCS contractors undertaking the supply, design. Installation, set to work commissioning and handover of micro and small wind turbine systems* [Online], London, Microgeneration Certification Scheme. Available at http://www.microgenerationcertification.org/images/MIS_3003_Issue_3.4_Micro_Wind.pdf (Accessed 20 March 2017).

Musgrove, P. J. (1990) 'Vertical axis WECS design' in Freris, L. L. (1990) *Wind Energy Conversion Systems*, Prentice Hall.

Musial, W., Heimiller, D., Beiter, P., Scott, G. and Draxi, C. (2016) *2016 Offshore Wind Energy Resource for the United States*, Colorado, National Renewable Energy Laboratory.

NATS (2016) *Self-assessment maps*, [Online]. Available at http://www.nats.aero/services/information/wind-farms/self-assessment-maps/ (Accessed 1 March 2017).

Natural England (2009a) Technical Information Note TIN051: *Bats and onshore wind turbines – Interim guidance*, Worcester, Natural England.

Natural England (2009b) Technical Information Note TIN059: *Bats and single large wind turbines: Joint Agencies interim guidance*, Worcester, Natural England.

Natural England (2010) Technical Information Note TIN069: *Assessing the effects of onshore wind farms on birds*, Worcester, Natural England.

Needham, J. (1965) *Science and Civilisation of China*, Cambridge, Cambridge University Press.

NERI (1998) *Impact Assessment of an Off-shore Wind Park on Sea Ducks, Technical Report No. 227*, Denmark, National Environmental Research Institute (NERI).

NOP (2005) *Survey of Public Opinion of Wind Farms*, NOP (National Opinion Poll (UK)

NPL (2016) *Wind turbine Noise Model*, [Online]. Available at http://resource.npl.co.uk/acoustics/techguides/wtnm/ (Accessed 13 December 2016).

NRC (2007) *Environmental Impacts of Wind Energy Projects, Committee on Environmental Impacts on Wind Energy*, Washington DC, National Academies Press.

NWCC (2007) *NWCC Mitigation toolbox*, Washington, National Wind Coordinating Collaborative.

NWCC (2011) *Comprehensive Guide to Studying Wind Energy/Wildlife Interactions*, Washington, National Wind Coordinating Collaborative.

ODPM (2004a) *Planning Policy Statement 22 (PPS22): Renewable Energy*, Norwich, Office of the Deputy Prime Minister.

ODPM (2004b) *Planning for Renewable Energy – A Companion Guide to PPS22*, Norwich, Office of the Deputy Prime Minister.

Ofcom (2009) *Tall structures and their impact on broadcast and other wireless services*, https://www.ofcom.org.uk/__data/assets/pdf_file/0026/63494/tall_structures.pdf (Accessed 20 March 2017).

Ofcom (2017) *Fixed terrestrial links: Windfarms and Wireless Services: Coordination and Guidance*, [Online]. Available at https://www.ofcom.org.uk/manage-your-licence/radiocommunication-licences/fixed-terrestrial-links (Accessed 1 March 2017).

ORE-Catapult (2016) *SPARTA: The performance data exchange platform for offshore wind*, [Online], Glasgow, Catapult and London, The Crown Estate. Available at https://ore.catapult.org.uk/our-services/ (Accessed 1 March 2017).

ORE-Catapult (2017) Operations & Maintenance (O&M). Offshore Renewable Energy (ORE) Catapult, https://ore.catapult.org.uk/our-services/innovation-challenges/offshore-wind-innovation-challenges/operations-mantenance (Accessed 9 January 2017).

OVG (2010) *the Offshore Valuation – A valuation of the UK's offshore renewable energy resource*, [Online], Offshore Valuation Group and Public Interest Research Centre. Available at http://publicinterest.org.uk/offshore/downloads/offshore_valuation_exec.pdf (Accessed 1 March 2017).

PB (2011) *Update of UK Shadow Flicker Evidence Base – Final Report*, Newcastle Upon Tyne, Parsons Brinckerhoff.

Planning Guidance (2015) *Renewable and low carbon energy: Particular planning considerations for hydropower, active solar technology, solar farms and wind turbines*, Planning Guidance, Department of Communities and Local Government, available at https://www.gov.uk/guidance/renewable-and-low-carbon-energy#particular-planning-considerations-for-hydropower-active-solar-technology-solar-farms-and-wind-turbines (Accessed 19 March 2017).

Randhawa, B. S. and Rudd, R. (2009) *RF Measurement Assessment of Potential Wind Farm Interference to Fixed links and Scanning telemetry Devices, ERA Report Number 2008-0568* Leatherhead, Surrey, ERA Technology Ltd for Ofcom.

RenewableUK (2010a) *Wind Energy Generation Costs, Fact Sheet 04, June*, [Online], London, RenewableUK. Available at http://www.solarventus-energy.co.uk/Wind-Energy-Generation-Costs.pdf (Accessed 1 March 2017).

RenewableUK (2010b) *Onshore Costs/Benefit Study*, London, RenewableUK.

RenewableUK (2011a) *Planning Guidance: Small Wind – A good practice guide*, [Online], London. Available at http://www.caithnesswindfarms.co.uk/Small%20wind.pdf (Accessed 1 March 2017).

RenewableUK (2011b) *Planning Guidance: Small Wind – Appendices*, London, RenewableUK. Available at Available at https://c.ymcdn.com/sites/renewableuk.site-ym.com/resource/resmgr/publications/guides/small_wind_planning_a.pdf (Accessed 20 March 2017).

RenewableUK (2014) *Small Wind Turbine Standard*, London, RenewableUK. Available at http://smallwindcertification.org/wp-content/uploads/2014/08/RUK-Small-Wind-Turbine-Standard3.pdf (Accessed 20 March 2017)

RenewableUK (2015) *Guidance & Supporting Procedures on the Application of Wind Turbine Safety Rules*, London, RenewableUK. RenewableUK Available at http://c.ymcdn.com/sites/www.renewableuk.com/resource/collection/ae19eca8-5b2b-4ab5-96c7-ecf3f0462f75/Wind-turbine-safety-rules-guidance.pdf?hhSearchTerms=%22small+and+wind+and+turbine+and+standard%22 (Accessed 20 March 2017)

RenewableUK (2016a) *Offshore Renewables Aviation Guidance (ORAG); Good Practice Guidelines for Offshore Renewable Energy Developments*, London, RenewableUK. Available at http://c.ymcdn.com/sites/renewableuk.site-ym.com/resource/resmgr/publications/reports/orag_aviationguidance.pdf (Accessed 20 March 2017).

RenewableUK (2016b) *New records set in best ever year for British wind energy generation*, London, RenewableUK. Available at http://c.ymcdn.com/sites/renewableuk.site-ym.com/resource/resmgr/publications/reports/orag_aviationguidance.pdf (Accessed 20 March 2017).

RenewableUK (2017) UK wind speed database [Online]. Available at http://www.bwea.org/noabl/ (Accessed 1 March 2017).

Reynolds, J. (1970) *Windmills and Watermills*, London, Hugh Evelyn Ltd Publishers.

Risø (2009) *European wind resources over open sea*, [Online]. Available at http://www.windatlas. dk/europe/oceanmap.html (Accessed 9 November 2011).

Rodrigues, L. et al. (2014) *Guidelines for consideration of bats in wind farm projects*, Revision 2014, EUROBATS Publication Series No. 6. Available at www.eurobats.org/sites/default/files/documents/publications/publication_series/pubseries_no6_english.pdf (Accessed 20 July 2017).

Rogers, A. L., Rogers, J. W. and Manwell, J. F. (2005) 'Comparison of the Performance of Four Measure-Correlate-Predict Algorithms', *Journal of Wind Engineering and Industrial Aerodynamics*, vol. 93, no. 3, pp. 243–264.

Rogers, A. L., Rogers, J. W., Manwell, J. F. (2006a) 'Uncertainties in Results of Measure-Correlate-Predict Analysis', *European Wind Energy Conference*, February/March.

Rogers, A. L., Manwell, J. F., Wright, S. (2006b) *Wind turbine Acoustic Noise – A White Paper*, Amherst, Renewable Energy Research Laboratory, University of Massachusetts.

Van Rooij, R. and Timmer, N. (2004) *Design of Airfoil for Wind turbine Blades*, The Netherlands, Delft University of Technology.

RSPB (2015) *UK Onshore Bird Sensitivity Map*, [Online]. Available at http://www.rspb.org.uk/Images/Onshore_wind_sensitivity_2015_tcm9-432921.pdf (Accessed 1 March).

RSPB (2016a) *Lodge wind turbine*, [Online]. Available at http://www.rspb.org.uk/reserves-and-events/find-a-reserve/reserves-a-z/reserves-by-name/t/thelodge/windturbine/index.aspx (Accessed 1 March 2017).

RSPB (2016b) *The RSPB's 2050 energy vision: Meeting the UK's climate targets with nature*, [Online], Sandy, Bedfordshire, Royal Society for the Protection of Birds. Available at www.rspb.org.uk/images/energy_vision_summary_report_tcm9-419580.pdf (Accessed 1 March 2017).

SDC (2005) *Wind Power in the UK: A guide to key issues surrounding wind power development in the UK* [Online]. Available at https://research-repository.st-andrews.ac.uk/handle/10023/2306 (Accessed 1 March 2017).

Smith, A., Stehly, T. and Musail, W. (2015) *2014-2015 Offshore Wind Technologies Market Report, Technical Report NREL/TP-5000-64283* Colorado, National Renewable Energy Laboratory.

South, P. and Rangi, R. (1972) *Wind tunnel investigation of a 14 feet diameter vertical axis windmill, Report Number LTR-LA-105*, Ontario, Canada, National Aeronautical Establishment, National Research Council.

Stiedal, H (2014) *Innovate to Generate – Making Offshore Wind a Truly Global Energy Source* [Online], London, Carbon Trust. Available at https://www.carbontrust.com/media/571800/carbon-trust-innovate-to-generate-18-09-14.pdf (Accessed 1 March 2017).

Sutherland, H. J., Berg, D. E. and Ashwill, T. D. (2012) *A Retrospective of VAWT Technology*, Albuquerque, New Mexico, Sandia National Laboratories.

Tangler, J. L. and Somers, D. M. (1995) *NREL Airfoil Families for HAWTs*, Colorado, National Renewable Energy Laboratory.

Taylor, D. A. (1998) 'Using buildings to harvest wind energy' in *Building Research and Information*, E & FN Spon.

TNEI (2007) *Onshore Wind Energy Planning Conditions Guidance Note, A report for the Renewables Advisory Board and BERR*, Newcastle, TNEI Services Ltd.

Troen, I. and Lundtang Petersen, E. (1989) *European Wind Atlas*, Roskilde, Risø National Laboratory.

Udell, D., Infield, D. and Watson, S. (2010) 'Low-cost mounting arrangements for building-integrated wind turbines', *Wind Energy*, vol. 13, no. 7, pp. 657–669.

US DOE (2015) *Wind Vision: A New Era for Wind Power in the United States*, Washington, US Department of Energy.

USFWS (2010) *Wind turbine Guidelines Advisory Committee – Recommended Guidelines*, Washington, US Fish and Wildlife Service.

USFWS (2012) *Land-Based Wind Energy Guidelines*, [Online], Washington, US Fish and Wildlife Service. Available at https://www.fws.gov/ecological-services/es-library/pdfs/WEG_final.pdf (Accessed 1 March 2017).

VertAx (2017) *VertAx Wind Ltd* [Online]. Available at http://vertaxwind.com/ (Accessed 2 March 2017).

VPM (2017) *VAWTPower Management, Inc.* [Online]. Available at http://www.vawtpower.blogspot.co.uk/ (Accessed 2 March 2017).

WEC (2016) *World Energy Resources: Wind 2016*, London, World Energy Council.

WEF (2017) *Renewable Infrastructure Investment Handbook: A Guide for Investors*, [Online], Cologny, Geneva, Switzerland, World Economic Forum. Available at www3.weforum.org/docs/WEF_Renewable_Infrastructure_Investment_Handbook.pdf (Accessed 2 March 2017).

Westmill Wind Farm Co-operative (2017) *Westmill Wind Farm Co-operative* [Online]. Available at http://www.westmill.coop/ (Accessed 2 March 2017).

WHO (2014) *Burden of disease from Household Air Pollution for 2012*, Geneva, Switzerland, World Health Organization.

WHO (2016) *Air Pollution. A global assessment of exposure and burden of disease*, Geneva, Switzerland, World Health Organization.

Willow, C. and Valpy, B. (2011) *Offshore Wind – Forecasts of future costs*, Cricklade, Swindon, Wiltshire, BVG Associates for RenewableUK.

Wolfram (2011) The *Wolframs Demonstrations Project demonstration of 2D Vector Addition*, [Online]. Available at http://demonstrations.wolfram.com/2DVectorAddition/ (Accessed 2 March 2017).

YouGov (2010) *Public Attitudes to Wind Farm YouGov Survey*, London, YouGov plc for Scottish Renewables.

Zervos, A. and Kjaer, C. (2009) *Pure Power – Wind energy targets for 2020 and 2030*. Brussels, European Wind Energy Association.